Technical Report 2, Part III

AN EXAMINATION OF SELECTED HF PHASE MODULATION TECHNIQUES

By: N. T. GAARDER

Prepared for:

U.S. ARMY RADIO PROPAGATION AGENCY
FORT MONMOUTH, NEW JERSEY

CONTRACT DA 36-039 SC-90859

STANFORD RESEARCH INSTITUTE

MENLO PARK, CALIFORNIA

STANFORD RESEARCH INSTITUTE
MENLO PARK, CALIFORNIA

February 1965

Technical Report 2, Part III

AN EXAMINATION OF SELECTED HF PHASE MODULATION TECHNIQUES

Prepared for:

U.S. ARMY RADIO PROPAGATION AGENCY
FORT MONMOUTH, NEW JERSEY

CONTRACT DA 36-039 SC-90859

By: N. T. GAARDER

SRI Project 4172

Approved: W. R. VINCENT, MANAGER
COMMUNICATION LABORATORY

D. R. SCHEUCH, EXECUTIVE DIRECTOR
ELECTRONICS AND RADIO SCIENCES

Copy No. .....6...

CONTENTS

ILLUSTRATIONS

TABLES

I INTRODUCTION

This report develops a probability-of-binary-error expression for a basic binary-adaptive-phase-shift-keyed (BAPSK) system. The error-rate expression uses the mathematical BAPSK system model developed in Technical Report 2, Part I on this contract[1]† and a mathematical propagation-medium model of the type discussed in Technical Report 2, Part II.[2] After the probability-of-error expression for a basic BAPSK system has been developed, this expression is modified to include various BAPSK modifications (time guard band, diversity, delay compensation, and others).

The propagation-medium model used in the error-rate expression, which specifically models the high-frequency (HF) propagation medium, is discussed and related to the HF propagation medium. The propagation-medium model includes additive noise, and thus it models the additive as well as the dispersive corruption of the HF propagation medium.

Because the error-rate expression developed in this report is relatively simple, the probability of error for a basic BAPSK system is plotted as a function of the signal-to-noise (S/N) for many types of dispersive channels. The most significant feature of the error-rate curves is that the probability of error approaches an asymptotic nonzero value for high S/N. This asymptotic value is determined by the time-delay and frequency-shift structure of the propagation medium. By using this asymptotic value of the probability of error, the sensitivity of the basic BAPSK system's error rate to time delays and frequency shifts is analyzed.

By using the results of Technical Report 3,[3] a basic BAPSK system is compared with a basic binary-differential-phase-shift-keyed (BDPSK) and quaternary-differential-phase-shift-keyed (QDPSK) systems. The error-rate performance of a BAPSK system is found to be degraded by frequency shifts much more than that of either a BDPSK system or a QDPSK system; however, at low S/N, a BAPSK system outperforms BDPSK and QDPSK systems. The performance of a BAPSK system and that of a BDPSK system are equally sensitive to time-delay effects.

---

†References are given at the end of the report.

II THE PROPAGATION-MEDIUM MODEL

This report uses a propagation-medium model of the type discussed by Stein,[4] Bello,[5] and Daly[2] to model the dispersive corruption of the propagation medium. However, the model used in the error-rate analysis is specifically related to the HF propagation medium. This model also includes additive, white, Gaussian noise to model the additive corruption of the propagation medium.

The output of the propagation-medium model (see Fig. 1), $y(t)$ [$\mathbf{y}(t)$ is the complex representation of the real-valued output† $y(t)$], is assumed to be the sum of an additive noise, $\mathbf{n}(t)$, and the output of a random time-varying linear filter, $\mathbf{z}(t)$:

$$\mathbf{y}(t) = \mathbf{z}(t) + \mathbf{n}(t) \quad . \tag{1}$$

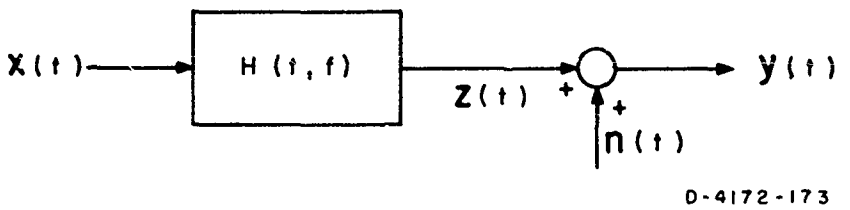

FIG. 1 BLOCK DIAGRAM OF PROPAGATION-MEDIUM MODEL

The additive noise, $\mathbf{n}(t)$, is assumed to be a zero-mean, stationary, white complex§ Gaussian random process:

$$\mathcal{E}[\mathbf{n}(t)] = 0 \tag{2}$$

---

† Throughout this report the complex representation for real processes discussed in Ref. 1 is used.

§ In this report all complex random fields, processes, and variables are implicitly assumed to have identically distributed (but not necessarily statistically independent) real and imaginary parts. All random variables are implicitly assumed to have statistically independent real and imaginary parts.

$$S_n(f) = \int_{-\infty}^{\infty} \mathcal{E}[\mathbf{n}(t)\mathbf{n}^*(t+\Delta t)] \exp\{-i2\pi f\Delta t\}\, d\Delta t$$
$$= \begin{cases} N_0, & f \geq 0 \\ 0, & f < 0 \end{cases} \qquad (3)$$

where $S_n(f)$ is the power spectral density of the noise, N_0 is the noise power per unit bandwidth, $\mathbf{n}^*$ is the complex conjugate of $\mathbf{n}$, and $\mathcal{E}[\cdot]$ is the usual expectation operator. The use of a zero-mean, stationary, white, complex Gaussian random process to model the additive noise has been well justified.[6]

The output of the time-varying linear filter

$$\mathbf{z}(t) = \int_{-\infty}^{\infty} \mathbf{H}(t,f)\mathbf{X}(f) \exp(i2\pi ft)\, df \quad , \qquad (4)$$

where the Fourier transform of the channel input,

$$\mathbf{X}(f) = \int_{-\infty}^{\infty} \mathbf{x}(t) \exp(-i2\pi ft)\, dt \quad , \qquad (5)$$

and the time-varying transfer function of the filter, $\mathbf{H}(t,f)$, accounts for the time and frequency scattering of the input energy. The time-varying transfer function, $\mathbf{H}(t,f)$, is assumed to be a zero-mean, homogeneous, complex Gaussian random field. Because the transfer function is a complex zero-mean, homogeneous, Gaussian random field, its statistics, and the statistics of its output for a known input are completely determined by the covariance function of the time-varying transfer function,

$$R_H(\Delta t,\Delta f) = \mathcal{E}[\mathbf{H}(t,f)\mathbf{H}^*(t+\Delta t, f+\Delta f)] \quad . \qquad (6)$$

This model for a time-varying radio channel has been justified by Stein,[4] Bello,[5] and Daly.[2] To model the HF propagation medium, it is necessary only to select an appropriate covariance function for the homogeneous time-varying transfer function or, equivalently, an appropriate scattering function,

$$S_H(\lambda,\tau) = \int_{-\infty}^{\infty}\int_{-\infty}^{\infty} R_H(\Delta t,\Delta f) \exp(i2\pi[-\lambda\Delta t + \tau\Delta f])\, d\Delta t\, d\Delta f \quad , \qquad (7)$$

for the time-varying filter.

It is well known that the HF propagation medium scatters energy discretely in time. This HF phenomenon, commonly referred to as multipath, is readily evidenced by the records of short-pulse oblique-incidence ionosphere sounder links.[7] The receivers on such links commonly detect several short pulses for each short pulse transmitted. These detected pulses are of different strengths and arrive at different times. The strengths and particularly the time displacements can be shown to correspond to various paths or modes of propagation. A suitable model to explain this multipath phenomenon only is a medium consisting of several paths each with a distinct time delay, gain, and phase shift. The output of such a medium,

$$\begin{aligned} \mathbf{y}(t) &= \sum_{k=1}^{K} a_k \exp(i\theta_k)\, \mathbf{x}(t - \tau_k) \\ &= \sum_{k=1}^{K} \mathbf{a}_k \mathbf{x}(t - \tau_k) \quad , \end{aligned} \tag{8}$$

where $\mathbf{x}(t)$ is the input to the medium, K is the number of paths, τ_k is the time delay of the kth path,

$$\mathbf{a}_k = a_k \exp(i\theta_k) \tag{9}$$

is the complex gain of the kth path, a_k is the gain of the kth path, and θ_k is the phase shift of the kth path. If it is assumed that for each path $\mathbf{a}_k$, the complex gain, is a zero-mean, complex Gaussian random variable† with variance

$$\mathcal{E}[|\mathbf{a}_k|^2] = \sigma_k^2 \quad , \tag{10}$$

the strength of the kth path, and that the complex gains of all the paths are statistically independent, then the propagation medium is equivalent to a zero-mean, homogeneous, (time-invariant) Gaussian random filter with covariance function,

$$R_H(\Delta t, \Delta f) = \sum_{k=1}^{K} \sigma_k^2 \exp(i2\pi\Delta f \tau_k) \tag{11}$$

† The assumption that the complex gain of each path is a (complex) zero-mean Gaussian random variable is equivalent to the assumption that the gain of each path is a Rayleigh random variable with mean, $\mathcal{E}[a_k] = (\sqrt{\pi}/2)\sigma_k$ and that the phase shift of each path is uniformly distributed on the interval $[0, 2\pi)$.

$$R_{\mathbf{H}}(\Delta t,\Delta f) = \sum_{k=1}^{K} \sigma_k^2 \exp\ (i2\pi\Delta f\tau_k) \tag{11}$$

and thus scattering function

$$S_{\mathbf{H}}(\lambda,\tau) = \sum_{k=1}^{K} \sigma_k^2\ \delta(\tau - \tau_k)\delta(\lambda) \quad . \tag{12}$$

Such a time-invariant model for the HF propagation medium (consisting of energy scattering in time only) is unrealistic, because even though it accounts for frequency-selective fading and intersymbol interference, it does not account for time-selective fading, for interchannel interference caused by the propagation-medium scattering energy in frequency, or for the continual change of the gain and phase of the propagation medium with time. Perhaps the best example of the presence of energy scattering in frequency occurs when a CW tone transmitted over an HF link is envelope-detected. The variations (in time) of the level of the envelope-detector output (a phenomenon referred to as time-selective fading) can be caused only by the propagation medium scattering the input energy in frequency. If the propagation medium did not scatter energy in frequency, the level of the envelope detector output would not change with time. Thus a comprehensive model of the HF propagation medium must incorporate energy scattering in frequency as well as in time.

The exact nature of energy scattering in frequency does not appear to be well known; recent work at Stanford Research Institute,[8,9] seems to indicate that the HF propagation medium tends to scatter energy in discrete packets in frequency as well as in time. That is, the propagation medium tends to shift the input energy by several distinct (Doppler) frequencies.

The HF propagation-medium model used in the error-rate analysis consists of several paths, each path having a distinct complex gain (gain and phase shift), time delay, and frequency shift. The output of such a medium,

$$\mathbf{y}(t) = \sum_{k=1}^{K} \mathbf{a}_k \exp\ (i2\pi\lambda_k t)\ \mathbf{x}\ (t - \tau_k)\ , \tag{13}$$

where $\mathbf{x}(t)$ is the input to the medium, K is the number of paths, λ_k is the frequency shift, τ_k is the time delay, and $\mathbf{a}_k = a_k e^{i\theta_k}$ is the complex

gain (a_k is the gain and θ_k is the phase shift) of the kth path. It is again assumed that for each path the complex gain, $\mathbf{a}_k$, is a zero-mean, complex, Gaussian random variable with variance

$$\mathcal{E}[|\mathbf{a}_k|^2] = \sigma_k^2 \quad , \tag{14}$$

equal to the strength of the kth path, that the time delay, τ_k, is known, that the frequency shift, λ_k, is known, and that the complex gains of all the individual paths are statistically independent of each other. Under these assumptions, the propagation-medium model is equivalent to a zero-mean, homogeneous, Gaussian random filter with covariance function

$$R_H(\Delta t, \Delta f) = \sum_{k=1}^{K} \sigma_k^2 \exp\left(-i2\pi[\lambda_k \Delta t - \tau_k \Delta f]\right) \tag{15}$$

and thus scattering function

$$S_H(\lambda, \tau) = \sum_{k=1}^{K} \sigma_k^2 \delta(\lambda - \lambda_k)\delta(\tau - \tau_k) \quad . \tag{16}$$

Note that the propagation-medium model can be made frequency-invariant (*i.e.*, purely time-selective) by setting all the τ_k to zero, time-invariant (*i.e.*, purely frequency-selective) by setting all the λ_k to zero, and time- and frequency-invariant (*i.e.*, flat-flat fading) by setting all the τ_k and λ_k to zero. In addition, by making K very large, a continuous scattering function can be closely approximated. In analyzing the sensitivity of various systems to time delays and frequency shifts, it will be convenient to consider time-invariant, frequency-invariant, and time-and-frequency-invariant propagation mediums. Time-and-frequency-invariant propagation mediums have been extensively studied by many authors.[10,11,12] In the literature, the time-and-frequency-invariant propagation medium model is referred to as the flat-flat Rayleigh fading channel model.

For a better understanding of the effects of time delays and frequency shifts upon transmitted signals, a particular propagation-medium model is now discussed in more detail. This particular model, which is typical of many HF channels for reasonable time intervals, consists of two paths each with a distinct and constant time delay, frequency shift, and complex gain. Let the input to the propagation medium be a CW tone at

an arbitrary frequency, f. If this signal is denoted by its complex representation,

$$\mathbf{x}(t,f) = \exp(i2\pi ft) \quad ; \tag{17}$$

the output of the propagation medium (neglecting additive noise),

$$\mathbf{y}(t,f) = \mathbf{a}_1 \exp(i2\pi[f-\lambda_1][t-\tau_1]) + \mathbf{a}_2 \exp(i2\pi[f-\lambda_2][t-\tau_2]) \quad , \tag{18}$$

where $\mathbf{a}_k$ is the complex gain, τ_k is the time delay, and λ_k is the frequency shift of the kth path. If the output of the propagation medium is envelope-detected, the output of the envelope detector,

$$|\mathbf{y}(t,f)|^2 = |\mathbf{a}_1|^2 + |\mathbf{a}_2|^2 + 2|\mathbf{a}_1|\cdot|\mathbf{a}_2| \cos(2\pi[f\Delta\tau + t\Delta\lambda] + \Delta\phi) \quad , \tag{19}$$

where the differential frequency shift, $\Delta\lambda = \lambda_2 - \lambda_1$, the differential time delay, $\Delta\tau = \tau_2 - \tau_1$, and the differential phase shift,

$$\Delta\phi = \lambda_1\tau_1 - \lambda_2\tau_2 - \cos^{-1}\left(\frac{\mathbf{a}_1\mathbf{a}_2^*}{|\mathbf{a}_1||\mathbf{a}_2|}\right) \quad .$$

Thus the output of the envelope detector is at a relative minimum (*i.e.*, in a fade) when $\cos[2\pi(f\Delta\tau + t\Delta\lambda) + \Delta\phi] = -1$ or, equivalently,

$$\Delta\lambda t_F + \Delta\tau f_F = \pm n + \frac{1}{2} - \frac{\Delta\phi}{2\pi} \tag{20}$$

for some integer n; the subscript F denotes that a fade occurs at that particular time and frequency.

In a time-frequency space, the set of points (fade coordinates) satisfying Eq. (20) is a series of parallel straight lines, with each integer n determining one straight line of the series. Figure 2 is a plot of a typical set of fade coordinates.

At any fixed time, t_0, the fades are spaced in frequency by $1/\Delta\tau$, the reciprocal of the differential time delay. At any fixed frequency, f_0, the fades are spaced in time by $1/\Delta\lambda$, the reciprocal of the differential frequency shift. In addition, at any particular time, t_0, the output

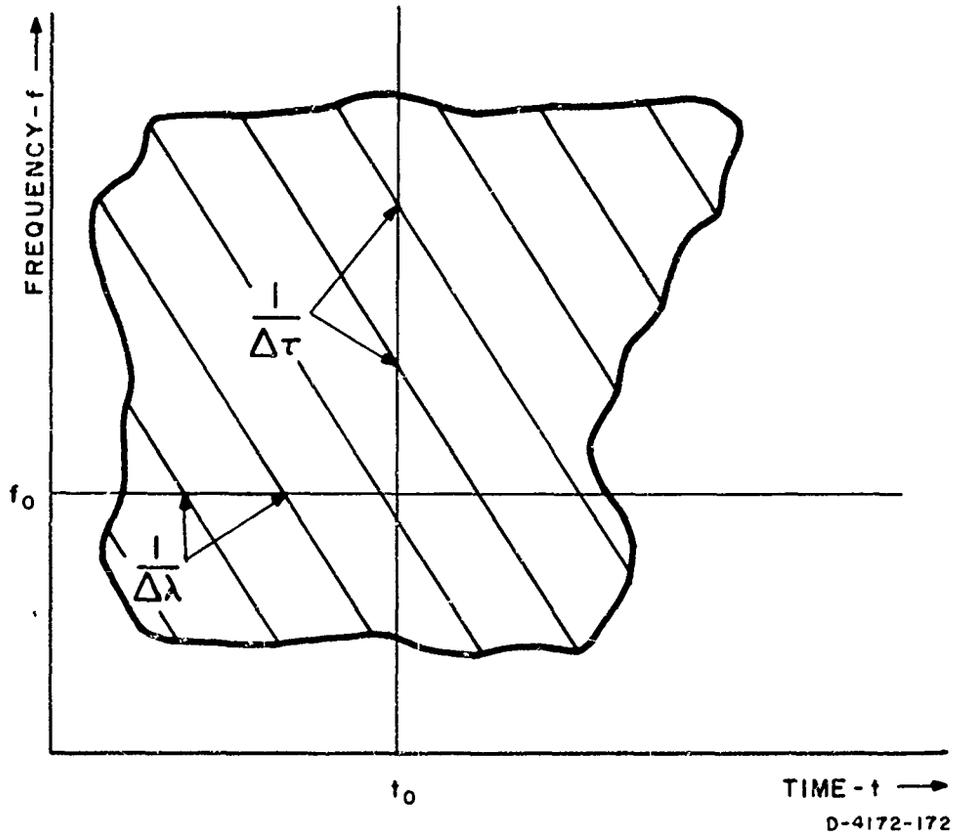

FIG. 2 TYPICAL FADE COORDINATES

of the envelope detector,

$$|\mathbf{y}(t_0, f)|^2 = |\mathbf{a}_1|^2 + |\mathbf{a}_2|^2 + 2|\mathbf{a}_1| \cdot |\mathbf{a}_2| \cos(2\pi f \Delta\tau + \theta_0) \quad , \quad (21)$$

where $\theta_0 = \Delta\phi + 2\pi\Delta\lambda t_0$. At any particular frequency, f_0 the output of the envelope detector is again of the same form as Eq. (19), since

$$|\mathbf{y}(t, f_0)|^2 = |\mathbf{a}_1|^2 + |\mathbf{a}_2|^2 + 2|\mathbf{a}_1| \cdot |\mathbf{a}_2| \cos(2\pi\Delta\lambda t + \phi_0) \quad ,$$

where $\varphi_0 = \Delta\phi + 2\pi f_0 \Delta\tau$.

The results of this digression can be extended to a more general propagation medium; however, the spacing of fades in frequency at a fixed time is still determined primarily by the time delays of the paths, and the spacing of fades in time at a fixed frequency is still determined by the frequency shifts of the paths.

This discussion has been partially verified experimentally by Ames.[13] The experiment consisted of transmitting a frequency-modulated signal over an HF link and simultaneously determining the time-delay structure of the link by using an oblique-incidence ionosphere sounder. The received signal was envelope-detected and spectrum-analyzed, and the output of the spectrum analyzer was plotted as intensity in a time-frequency space. When the propagation medium consisted of two paths, the points of minimum intensity (*i.e.*, fades) formed straight lines similar to those in Fig. 2. In addition, at any fixed time, the frequency spacing between (frequency-) selective fades was $1/\Delta\tau$, the reciprocal of the differential time delay. It was also found that at a fixed frequency the spacing in time between (time-) selective fades was constant, but not correlated with $1/\Delta\tau$. Because no measurement of frequency shifts was made in the experiment, the time spacing between (time-) selective fades could not be correlated with the differential frequency shift.

In an extension of his work, Ames considered fade patterns in a position and time space.[14] The fade patterns in the position-and-time experiment were similar to the fade patterns in the time-and-frequency experiment. The latter experiment indicated that, in general, most space-diversity antennas are not uncorrelated. Because of the increased complexity in the mathematical models necessary to model these effects (a scattering function of many more dimensions and the position and polarization of the diversity antennas), the error-rate analysis considers only (space-) diversity antenna outputs that are either completely correlated (identical) or completely uncorrelated (independent). It was felt that with this approach the performance of systems using (space-) diversity outputs that were neither completely correlated nor completely uncorrelated could be approximated. In addition, the error rate is bounded above by the error rate for identical space-diversity antenna outputs.

To summarize the propagation-medium model: the output of the model is

$$\mathbf{y}(t) = \int_{-\infty}^{\infty} \mathbf{H}(t,f)\mathbf{X}(f) \exp(i2\pi ft)\, dt + \mathbf{n}(t) \quad , \qquad (23)$$

where $\mathbf{X}(f)$ is the Fourier transform of the input, $\mathbf{n}(t)$, is the additive noise which accounts for additive corruption effects, and $\mathbf{H}(t,f)$ is the time-varying transfer function of the channel which accounts for the ionospheric dispersive effects. The additive noise, $\mathbf{n}(t)$, is assumed to

be a stationary, zero-mean, complex, Gaussian random process with spectrum,

$$S_n(f) = \begin{cases} N_0, & f \geq 0 \\ 0, & f < 0 \end{cases} , \tag{3}$$

where N_0 is the noise power per unit bandwidth. The time-varying transfer function,

$$\mathbf{H}(t,f) = \sum_{k=1}^{K} \mathbf{a}_k \exp\left(i2\pi[f\tau_k - \lambda_k t]\right) , \tag{24}$$

where K is the number of paths, $\mathbf{a}_k$ is the complex gain, τ_k is the time delay, and λ_k is the frequency shift of the kth path, is a homogeneous, zero-mean, complex Gaussian random field with power spectral density (*i.e.*, scattering function),

$$S_{\mathbf{H}}(\lambda,\tau) = \sum_{k=1}^{K} \sigma_k^2 \delta(\lambda - \lambda_k)\delta(\tau - \tau_k) , \tag{16}$$

where σ_k^2 is the strength of the kth path. The complex gains, $\mathbf{a}_k$, are statistically independent, zero-mean, complex, Gaussian random variables with variance σ_k^2; the time delays, τ_k, frequency shifts, λ_k, and strengths, σ_k^2, are known, as well as the number of paths, K. Because of the special form of the time-varying transfer function, the output of the propagation medium can also be expressed as:

$$\mathbf{y}(t) = \sum_{k=1}^{K} \mathbf{a}_k \exp\left(i2\pi\lambda_k t\right) \mathbf{x}\left(t - \tau_k\right) + \mathbf{a}(t) . \tag{25}$$

The random filter and the additive noise are statistically independent.

III BAPSK SYSTEM PROBABILITY-OF-ERROR EXPRESSION

This section develops an expression for the probability of a binary error for a basic BAPSK system operating in the non-redundant mode. The output of a BAPSK system transmitter $\mathbf{x}(t)$, which is described in Sec. III of Ref. 1, is the input to the propagation-medium model discussed in the preceding section. The output of the propagation-medium model,

$$\mathbf{y}(t) = \sum_{k=1}^{K} \mathbf{a}_k \exp(i2\pi\lambda_k t)\, \mathbf{x}(t - \tau_k) + \mathbf{n}(t) \quad ,$$

is the input to a BAPSK system receiver, which is described in Sec. IV of Ref. 1.† Since the actual probability-of-error expression is complex and difficult to calculate (even with a digital computer), a convenient and accurate approximation to the probability of error is found. This approximation is valid for a wide range of systems other than a BAPSK system, and it greatly simplifies the computation of the probability of error. The probability-of-error expression considers errors caused by dispersive corruption (the variations in time and frequency of the complex gain of the propagation medium), additive corruption (the additive noise of the propagation medium), and inherent self-interference (the nonzero information-tone component of the long-term-average filter output). It does not consider other errors caused by implementative corruption (the malfunctioning of equipment).

From the results of Ref. 1, it is readily apparent that the nth subsystem of the BAPSK system will err in the transmission of the kth binary digit of the nth information sequence I_k^n, if, and only if, the kth binary digit of the nth estimated information sequence $\tilde{I}_k^n$ is not equal to I_k^n. Because both I_k^n and $\tilde{I}_k^n$ take only the values +1 and −1, the probability of error in the transmission of I_k^n,

† In Sec. IV of this report, modifications [Sec. VI of Ref. 1] to a BAPSK system and operation in the redundant mode are incorporated into the probability-of-error expression.

$$P^n_{e,k} = \Pr\{\text{error in the transmission of } I^n_k\} = \Pr\{I^n_k \tilde{I}^n_k = -1\} \quad . \tag{26}$$

From Eq. (93) of Ref. 1, one finds that the kth digit of the nth estimated information sequence (for a basic BAPSK system operating in the nonredundant mode),

$$\tilde{I}^n_k = \text{sgn}\left(C^n_k \text{ Re}\{i\bar{\mathbf{y}}^n(k)\mathbf{y}^{n*}(k)\}\right) \quad , \tag{27}$$

where C^n_k is the kth element of the nth binary code-tone sequence, the long-term-average filter output,

$$\bar{\mathbf{y}}^n(k) = \sum_{j=-\infty}^{k-1} P^n_j \mathbf{y}^n(j) \exp\left(\alpha T[j-k]\right) \quad , \tag{28}$$

the matched filter output,

$$\mathbf{y}^n(k) = \int_{-\infty}^{\infty} \mathbf{y}_\Delta(t) \exp\left(-i2\pi[f_n - \Delta]t\right) \rho\left(t - t_0 - kT\right) dt \quad , \tag{29}$$

$$\text{sgn}(x) = \begin{cases} +1 , & x \geq 0 \\ -1 , & x < 0 \end{cases} \quad , \tag{30}$$

and Re $\{\mathbf{x}\}$ denotes the real part of $\mathbf{x}$. In Eq. (28), P^n_j is the jth binary element of the nth pilot-tone sequence, α is the time constant of the long-term-average filter,† and $1/T$ is the signaling rate of the system. In Eq. (29),

$$\mathbf{y}_\Delta(t) = \exp\left(-i2\pi\Delta t\right) \mathbf{y}(t) \quad , \tag{31}$$

is the output of the propagation medium $\mathbf{y}(t)$, hetrodyned to a frequency Δ cps less than the transmitter output; f_n is the center frequency of the nth subsystem;

$$\rho(t) = \begin{cases} 1 , & t \in [-T/2 , T/2) \\ 0 , & t \notin [-T/2 , T/2) \end{cases} \quad ; \tag{32}$$

† If the long-term-average filter is implemented digitally in the BAPSK system, $e^{\alpha T}$ is constrained to take one of the values $(1 - 2^{-n})^{-1}$, where n is an integer.

and t_0 is the BAPSK system synchronization time. The probability of error can thus be expressed as:

$$P^n_{e,k} = \Pr\{I^n_k C^n_k \operatorname{Re}\{i\bar{\mathbf{y}}^n(k)\mathbf{y}^{n*}(k)\} < 0\} \quad , \tag{33}$$

or equivalently as:

$$P^n_{e,k} = \Pr\{I^n_k C^n_k \mathbf{Y}^* Q \mathbf{Y} < 0\} \quad , \tag{34}$$

where the column vector†

$$\mathbf{Y} = \begin{bmatrix} \bar{\mathbf{y}}^n(k) \\ \mathbf{y}^n(k) \end{bmatrix} \quad , \tag{35}$$

the row vector $\mathbf{Y}^*$ is the transpose and complex conjugate of $\mathbf{Y}$, and the Hermitian matrix

$$Q = \begin{bmatrix} 0 & i \\ -i & 0 \end{bmatrix} \quad . \tag{36}$$

The probability-of-error expression can also be expressed in the form:

$$P^n_{e,k} = \sum_{\xi_j \in \Xi} \Pr\{I^n_k C^n_k \mathbf{Y}^* Q \mathbf{Y} < 0 \,|\, \xi = \xi_j\} \Pr\{\xi = \xi_j\} \quad , \tag{37}$$

where the set Ξ consists of all possible system transmitter states ξ_j. Each system transmitter state, ξ_j, consists of one possible set of values for each element of every pilot-tone, code-tone, and information sequence. Since the set Ξ has an infinite number of possible transmitter states, the probability of error, as expressed in Eq. (37), is impossible to compute without further assumptions. This difficulty will be ignored for the moment, while the conditional probability of error for a given input state

$$P^n_{e,k}(\xi) = \Pr\{I^n_k C^n_k \mathbf{Y}^* Q \mathbf{Y} < 0 \,|\, \xi\} \tag{38}$$

† The superscript n and the argument k of the vector Y have been suppressed for simplicity.

is considered in more detail. This detailed consideration of the conditional probability of error eventually leads to an accurate approximation of the probability-of-error expression that essentially eliminates the infinite summation of Eq. (37).

When the transmitter state is known, the vector $\mathbf{Y}$ is a zero-mean, complex,† Gaussian random vector, because each of the components of the vector $\mathbf{Y}$ is the result of linear operations on the propagation-medium output $\mathbf{y}(t)$, which is the sum of two zero-mean, complex, Gaussian random processes. The statistics of the vector $\mathbf{Y}$, given the transmitter state, are thus completely determined by the Hermitian conditional covariance matrix;

$$K(\xi) = \mathcal{E}[\mathbf{Y}\mathbf{Y}^* | \xi] = \begin{bmatrix} k_{11}(\xi) & k_{12}(\xi) \\ k_{12}^*(\xi) & k_{22}(\xi) \end{bmatrix} , \tag{39}$$

where

$$k_{11}(\xi) = \mathcal{E}[|\overline{\mathbf{y}}^n(k)|^2 \ | \xi] , \tag{40}$$

$$k_{12}(\xi) = \mathcal{E}[\overline{\mathbf{y}}^n(k)\mathbf{y}^{n*}(k) \ | \xi] , \tag{41}$$

and

$$k_{22}(\xi) = \mathcal{E}[|\mathbf{y}^n(k)|^2 \ | \xi] . \tag{42}$$

It can be readily verified that there is a matrix $[K(\xi)]^{1/2}$ such that

$$K(\xi) = [K(\xi)]^{1/2}[K(\xi)]^{*/2} , \tag{43}$$

where $[K(\xi)]^{*/2}$ is the transpose and complex conjugate of $[K(\xi)]^{1/2}$. Now by assuming that the matrix $K(\xi)$ is nonsingular§ one finds that the vector

$$\mathbf{Z} = [K(\xi)]^{-1/2}\mathbf{Y} , \tag{44}$$

† All zero-mean, complex, random vectors considered in this report are implicitly assumed to have components with statistically independent, as well as identically distributed, real and imaginary parts. This assumption is consistent with the complex representation[1] used in this report. An immediate result of this assumption is that for any vector X, $\mathcal{E}[XX^T] = \phi$, the zero matrix (X^T is the transpose of X); thus the second-order statistics of X are completely determined by $\mathcal{E}[XX^*]$, the covariance matrix of the vector.

§ The probability-of-error expression developed here is applicable even when $K(\xi)$ is singular. The development of the probability-of-error expression is conceptually the same, but much longer, when $K(\xi)$ is singular; therefore this development is not included.

where $[K(\xi)]^{-1/2}$ denotes the inverse of $[K(\xi)]^{1/2}$, is a zero-mean, complex, Gaussian random vector with covariance matrix,

$$\mathcal{E}[\mathbf{Z}\mathbf{Z}^*|\xi] = [K(\xi)]^{-1/2}K(\xi)[K(\xi)]^{-*/2}$$

$$= \begin{bmatrix} 1 & 0 \\ 0 & 1 \end{bmatrix} = I \quad , \tag{45}$$

equal to the identity matrix. The conditional probability of error can now be expressed in terms of the vector $\mathbf{Z}$:

$$P^n_{e,k}(\xi) = \Pr\{\mathbf{Z}^* Q^n_k(\xi)\mathbf{Z} < 0\} \quad , \tag{46}$$

where the Hermitian matrix

$$Q^n_k(\xi) = I^n_k C^n_k [K(\xi)]^{*/2} Q [K(\xi)]^{1/2} \quad . \tag{47}$$

It is well known,[15] that there are matrices $\Lambda(\xi)$ and $P(\xi)$ such that:

$$Q^n_k(\xi) = P(\xi)^* \Lambda(\xi) P(\xi) \quad , \tag{48}$$

$$P(\xi)P(\xi)^* = I \quad , \tag{49}$$

and $\Lambda(\xi)$ is a diagonal matrix with the real-valued diagonal elements being the eigenvalues of the matrix $Q^n_k(\xi)$ [*i.e.*, the roots of the equation

$$|\lambda I - Q^n_k(\xi)| = 0 \quad , \tag{50}$$

where $|A|$ denotes the determinant of A]. Therefore the conditional probability of error,

$$P^n_{e,k}(\xi) = \Pr\{\mathbf{W}^* \Lambda(\xi) \mathbf{W} < 0\} \quad , \tag{51}$$

where the vector

$$\mathbf{W} = P(\xi)\mathbf{Z} \tag{52}$$

is a zero-mean, complex, Gaussian random vector with a covariance matrix equal to the identity matrix, I.

By expressing the conditional probability-of-error expression in terms of the components of the vector $\mathbf{W}$, $\mathbf{w}_1$, and $\mathbf{w}_2$, and the eigenvalues of the matrix $Q_k^n(\xi)$, $\lambda_1(\xi)$, and $\lambda_2(\xi)$, one finds that the conditional probability of error,

$$P_{e,k}^n(\xi) = \Pr\{\lambda_1(\xi)|\mathbf{w}_1|^2 + \lambda_2(\xi)|\mathbf{w}_2|^2 < 0\}$$

$$= \Pr\left\{\frac{|\mathbf{w}_1|^2}{|\mathbf{w}_2|^2} < -\frac{\lambda_2(\xi)}{\lambda_1(\xi)}\right\}$$

$$= \Pr\left\{f_2 < -\frac{\lambda_2(\xi)}{\lambda_1(\xi)}\right\} , \qquad (53)$$

where the random variable $f_2 = |\mathbf{w}_1|^2/|\mathbf{w}_2|^2$ is "F-distributed" with parameters $m = n = 2$.[16] The probability density of f_2,

$$p(f_2) = \begin{cases} (1 + f_2)^{-2} , & f_2 \geq 0 \\ 0 , & f_2 < 0 \end{cases} , \qquad (54)$$

and thus the conditional probability of error,

$$P_{e,k}^n(\xi) = \int_0^{-\lambda_2(\xi)/\lambda_1(\xi)} (1 + f_2)^{-2} df_2 = \frac{-\lambda_2(\xi)}{\lambda_1(\xi) - \lambda_2(\xi)} . \qquad (55)$$

The conditional probability-of-error expression implicitly assumes that $\lambda_1(\xi)$ and $-\lambda_2(\xi)/\lambda_1(\xi)$ are positive; to verify these assumptions one must compute the eigenvalues of $Q_k^n(\xi)$. The eigenvalues of $Q_k^n(\xi)$ satisfy Eq. (50); however,

$$|\lambda I - Q_k^n(\xi)| = |\lambda I - I_k^n C_k^n [K(\xi)]^{*/2} Q [K(\xi)]^{1/2}|$$

$$= |\lambda I - I_k^n C_k^n K(\xi) Q|$$

$$= \lambda^2 - \lambda I_k^n \text{ tr } [C_k^n K(\xi) Q] + |K(\xi) Q| , \qquad (56)$$

where tr $[A]$ denotes the trace of the matrix A. Noting that $|K(\xi)Q| = |K(\xi)||Q| = -|K(\xi)|$, one finds that

$$\lambda_1(\xi) = \frac{I_k^n \text{ tr } [C_k^n K(\xi) Q]}{2} \{1 + [1 + 4R^{-1}(\xi)]^{1/2}\} \quad , \tag{57}$$

$$\lambda_2(\xi) = \frac{I_k^n \text{ tr } [C_k^n K(\xi) Q]}{2} \{1 - [1 + 4R^{-1}(\xi)]^{1/2}\} \quad , \tag{58}$$

and the conditional probability of error,

$$P_{e,k}^n(\xi) = \frac{1}{2}\left\{1 - [1 + 4R^{-1}(\xi)]^{-1/2}\right\} \quad , \tag{59}$$

where the conditional hard-limiter input S/N

$$R(\xi) = \frac{\text{tr}^2 [K(\xi)Q]}{|K(\xi)|} \quad . \tag{60}$$

The assumption that $-\lambda_2(\xi)/\lambda_1(\xi)$ is nonnegative is equivalent to the assumption that $|K(\xi)| \geq 0$; however, $K(\xi)$ is a valid covariance matrix, and therefore $|K(\xi)| \geq 0$. Hence the assumption that $-\lambda_2(\xi)/\lambda_1(\xi)$ is nonnegative is valid.

The assumption that $\lambda_1(\xi)$ is positive is equivalent to the assumption that I_k^n tr $[C_k^n K(\xi)Q]$ is positive, but the trace of $C_k^n K(\xi)Q$ is the expected value (given the transmitter state) of the quantity $C_k^n \mathbf{Y}^* Q \mathbf{Y}$ which is compared with the zero threshold (*i.e.*, the input to the hard limiter) in the final stage of a BAPSK system receiver:

$$\text{tr } \{C_k^n K(\xi) Q\} = \mathcal{E}[C_k^n \mathbf{Y}^* Q \mathbf{Y} \mid \xi] \quad . \tag{61}$$

The kth element of the nth estimated information sequence, $\tilde{I}_k^n$, is +1, if $C_k^n \mathbf{Y}^* Q \mathbf{Y}$ is greater than zero; if $C_k^n \mathbf{Y}^* Q \mathbf{Y}$ is less than zero, then $\tilde{I}_k^n$ is -1. Obviously, if the system is to perform satisfactorily, $I_k^n \mathcal{E}[C_k^n \mathbf{Y}^* Q \mathbf{Y} | \xi] = I_k^n$ tr $[C_k^n K(\xi) Q]$ must be nonnegative. If I_k^n tr $[C_k^n K(\xi) Q]$ is negative, the conditional probability of error is greater than 1/2:

$$P_{e,k}^n(\xi) = \frac{1}{2}\{1 + [1 + 4R^{-1}(\xi)]^{-1/2}\} \quad , \quad \text{for} \quad I_k^n \text{ tr } [C_k^n K(\xi) Q] < 0 \quad . \tag{62}$$

A completely general expression for the conditional probability of error, which accounts for the unlikely event that I_k^n tr $[C_k^n K(\xi)Q]$ is negative, is

$$P_{e,k}^n(\xi) = \frac{1}{2}\{1 - \text{sgn}\,(I_k^n \text{ tr } [C_k^n K(\xi)Q])[1 + 4R^{-1}(\xi)]^{-1/2}\} \qquad (63)$$

For $P_{e,k}^n(\xi) < 1/4$, the conditional probability of error can be conveniently and accurately approximated by the inverse of the conditional output S/N:

$$P_{e,k}^n(\xi) \tilde{=} R^{-1}(\xi) = \frac{|K(\xi)|}{\text{tr}^2\,\{K(\xi)Q\}} \quad . \qquad (64)$$

Because large conditional probabilities of error result in a high unconditional system error rate, only values of $P_{e,k}^n(\xi) < 1/4$ are of interest for most practical applications. Thus, for practical applications, $R^{-1}(\xi)$ can be used as an accurate approximation to the conditional probability of error. It can be readily verified by inspection that $R^{-1}(\xi)$ is an upper bound on the conditional probability of error for $P_{e,k}^n(\xi) < 3/4$†; thus, with almost certainty, one can use $R^{-1}(\xi)$ as an upper bound on the conditional probability of error. This approximation to (or bound on) the conditional probability of error and the observation that $I_k^n \mathcal{E}[C_k^n \mathbf{Y}^* Q \mathbf{Y} | \xi] = I_k^n$ tr $\{C_k^n K(\xi)Q\}$ are employed in the mathematical justification of the approximation that alleviates the difficulties in the infinite summation of Eq. (37); an intuitive justification of the approximation is presented initially, however.

The (unconditional) probability-of-error expression for the basic BAPSK system as given by Eq. (37), can also be interpreted as an expectation over the transmitter state of the conditional probability of error:

$$P_{e,k}^n = \mathcal{E}[P_{e,k}^n(\xi)] \quad , \qquad (65)$$

where the transmitter state (*i.e.*, the values of all the binary, pilot-tone, code-tone, and information-sequence elements) is assumed to be random. The natural distribution to assume for the transmitter state is a Bernouli distribution—all the elements of all the sequences are statistically independent, and Pr $\{I_k^n = 1\}$ = Pr $\{P_k^n = 1\}$ = Pr $\{C_k^n = 1\} = 1/2$.

† Unfortunately, for $P_{e,k}^n(\xi) < 1/4$, $R^{-1}(\xi)$ is a poor approximation to the conditional probability of error.

This assumption, which is a standard assumption in almost all error-rate analyses, is made in this analysis also. An immediate result of this assumption is that the probability of error and conditional probability of error are independent of k; thus $P^n_{e,k}(\xi) = P^n_{e,0}(\xi) = P^n_e(\xi)$.

Because the expectation expressed in Eq. (65) is tremendously difficult to evaluate, it will be approximated. The probability-of-error approximation, $\tilde{P}^n_e$, which is essentially the approximation used in Ref. 3, is to replace $R^{-1}(\xi)$ by $\mathcal{E}[|K(\xi)|]/\mathcal{E}[\mathrm{tr}^2\,[K(\xi)Q]]$ in the conditional probability-of-error expression

$$\tilde{P}^n_e = \frac{1}{2}\left[1 - \left\{1 + 4\,\frac{\mathcal{E}[|K(\xi)|]}{\mathcal{E}[\mathrm{tr}^2\,[K(\xi)Q]]}\right\}^{-1/2}\right] . \tag{66}$$

This is an engineering approximation. It can also be intuitively justified for phase-shift-keyed systems: there exists an actual transmitter state, such that $\mathcal{E}[|K(\xi)|] = K(\xi_0)$, $\mathcal{E}[\mathrm{tr}^2\,[K(\xi)Q]] = \mathrm{tr}^2\,[K(\xi_0)Q]$, and thus P^n_e is the actual probability of error for a particular transmitter state.

In this report, the approximation is mathematically, as well as intuitively, justified for error probabilities of practical interest. For these values of the probability of error, the conditional probability of error is closely approximated by (and bounded above by, for $P^n_e(\xi) < 3/4$) $R^{-1}(\xi)$; thus the probability of error is closely approximated (and almost certainly bounded above) by

$$\mathcal{E}[R^{-1}(\xi)] = R^{-1} \tilde{=} P^n_e . \tag{67}$$

This expression for the probability of error is simpler to compute than Eq. (65); however, the computation is still difficult. The probability-of-error approximation used in this report (and in Ref. 3), P^n_e, can also be closely approximated for $P^n_e < 1/4$ (and bounded above for $P^n_e < 3/4$), by

$$\hat{R}^{-1} = \frac{\mathcal{E}[|K(\xi)|]}{\mathcal{E}[\mathrm{tr}^2\,[K(\xi)Q]]} . \tag{68}$$

Thus for error rates of practical interest, the expected value of $R^{-1}(\xi)$ is being approximated by $\mathcal{E}[|K(\xi)|]/\mathcal{E}[\mathrm{tr}^2\,[K(\xi)Q]]$; the ratio of the expected values of $|K(\xi)|$ and $\mathrm{tr}^2\,[K(\xi)Q]$

$$R^{-1} = \mathcal{E}\left[\frac{|K(\xi)|}{\mathrm{tr}^2\ [K(\xi)Q]}\right]$$

$$\approx \left[\frac{\mathcal{E}[|K(\xi)|]}{\mathcal{E}[\mathrm{tr}^2\ [K(\xi)Q]]}\right] = \tilde{R}^{-1} \quad . \tag{69}$$

The quantity $\mathrm{tr}^2\ [K(\xi)Q] = \mathcal{E}^2[C_k^n \mathbf{Y}^* Q \mathbf{Y}|\xi]$ is the expected value (given the input state) squared of the quantity compared with a zero threshold in the receiver; it is readily apparent that, if the system is performing satisfactorily, this quantity changes very little as the transmitter state changes:

$$\mathcal{E}^{1/2}[\sigma^2(\xi)] << \mathcal{E}[\mathrm{tr}^2\ [K(\xi)Q]] \quad , \tag{70}$$

where the variation in $\mathrm{tr}^2\ [K(\xi)Q]$,

$$\sigma(\xi) = \mathrm{tr}^2\ [K(\xi)Q] - \mathcal{E}[\mathrm{tr}^2\ [K(\xi)Q]] \quad . \tag{71}$$

The variations in $\mathrm{tr}^2\ [K(\xi)Q]$ will be primarily caused by the variations in the self-interference (dispersive interchannel and intersymbol interference and inherent self-interference). These changes resulting from the self-interference must obviously be much smaller than the "signal portion" of $\mathrm{tr}^2\ [K(\xi)Q]$ if the system is performing satisfactorily. The signal portion of $\mathrm{tr}^2\ [K(\xi)Q]$ does not change significantly, because the expectation over the propagation medium has removed all instantaneous fading and noise effects, and because the system is balanced—if self-interference effects are ignored, $\mathrm{tr}^2\ \{K(\xi)Q\}$ is essentially independent† of whether $I_0^n = +1$ or $I_0^n = -1$.

Because $\mathrm{tr}^2\ \{K(\xi)Q\}$ changes very little and $\mathrm{tr}^2\ [K(\xi)Q] >> 0$ $\mathcal{E}[|K(\xi)|]/\mathcal{E}[\mathrm{tr}^2\ [K(\xi)Q]]$ is a reasonable approximation to $\mathcal{E}[|K(\xi)|/\mathrm{tr}^2\ [K(\xi)Q]]$. For all values of practical interest, the probability of error is equal to

† The scattering function of the propagation medium must be symmetric about the origin for this to be strictly true (see Ref. 17).

$$R^{-1} = \mathcal{E}\left\{\frac{|K(\xi)|}{\mathcal{E}[\mathrm{tr}^2\ [K(\xi)Q]] + \sigma(\xi)}\right\}$$

$$= \frac{\mathcal{E}\{|K(\xi)|\}}{\mathcal{E}\{\mathrm{tr}^2\ [K(\xi)Q]\}} - \frac{\mathcal{E}\,[R^{-1}(\xi)\sigma(\xi)]}{\mathcal{E}\{\mathrm{tr}^2\ [K(\xi)Q\,]\}}$$

$$= \tilde{R}^{-1} - \frac{\mathcal{E}[R^{-1}(\xi)\sigma(\xi)]}{\mathcal{E}\{\mathrm{tr}^2\ [K(\xi)Q]\}} \qquad (72)$$

or, equivalently, the error in approximation

$$R^{-1} - \tilde{R}^{-1} = -\frac{\mathcal{E}[R^{-1}(\xi)\sigma(\xi)]}{\mathcal{E}\{\mathrm{tr}^2\ [K(\xi)Q]\}}\ , \qquad (73)$$

but by using the Schwartz inequality, one finds that

$$|R^{-1} - \tilde{R}^{-1}|^2 \leq \frac{\mathcal{E}[R^{-2}(\xi)]\,\mathcal{E}[\sigma^2(\xi)]}{\mathcal{E}\{\mathrm{tr}^2\ [K(\xi)Q]\}}\ . \qquad (74)$$

Thus the relative approximation error

$$\frac{|R^{-1} - \tilde{R}^{-1}|}{R^{-1}} \leq \frac{\overline{R^{-2}(\xi)}^{\,1/2}}{R^{-1}} \cdot \frac{\overline{\sigma^2}^{\,1/2}}{\mathcal{E}\{\mathrm{tr}^2\ [K(\xi)Q]\}}; \qquad (75)$$

however, $\overline{R^{-2}}^{1/2}/\overline{R^{-1}} < 1$ and $\overline{\sigma^2}^{1/2}/\mathcal{E}[\mathrm{tr}^2\ [K(S)Q]] \ll 1$. Thus the relative approximation error

$$\frac{|R^{-1} - \tilde{R}^{-1}|}{R^{-1}} < 1 \qquad (76)$$

for all values of interest. Because $P_e^n \cong R^{-1}$, the probability-of-error approximation is mathematically, as well as intuitively, justified for all practical values.

At this point, infinite summations are still present in the approximation; however, these summations can now be evaluated in closed form because only products, rather than products and ratios, of random variables are involved. Because the summations are relatively easy to

evaluate, the calculation of the probability of error is greatly simplified. This simplification is nontrivial, for as evidenced by the work of Bello,[18] the summations of Eq. (7) are quite difficult and tedious to evaluate.

Before proceeding with the evaluation of $\mathcal{E}[|K(\xi)|]$ and $\mathcal{E}[\mathrm{tr}^2\ [K(\xi)]]$, one should note that, although the probability-of-error expression has been developed for a basic BAPSK system, the expression is valid for many other binary communication systems as well. All binary communications systems† that compare a quadratic form $\mathbf{Y}^*Q\mathbf{Y}$, in (two complex) Gaussian random variables with a zero threshold to estimate each transmitted information digit, *i.e.*, $\tilde{I} = \mathrm{sgn}\ \{\mathbf{Y}^*Q\mathbf{Y}\}$, have a conditional probability of error

$$P_e(\xi) = \frac{1}{2}\{1 - \mathrm{sgn}\ [I_k^n\ \mathrm{tr}\ [K(\xi)Q]][1 + 4R^{-1}(\xi)]^{-1/2}\}$$

$$\tilde{=} R^{-1}(\xi), \qquad \text{for } P_e(\xi) < \frac{1}{4}\ , \tag{77}$$

where the conditional covariance matrix $K(\xi) = [\mathbf{Y}\mathbf{Y}^*|\xi]$, and ξ is the transmitter input state. The probability of error for such a system, $P_e = \mathcal{E}[P_e(\xi)]$, can be closely approximated by

$$\tilde{P}_e = \frac{1}{2}\{1 - \mathrm{sgn}\ (\mathcal{E}[I_k^n\ \mathrm{tr}\ [K(\xi)Q]])(1 + 4\tilde{R}^{-1})^{-1/2}\}\ ; \tag{78}$$

for the values of the probability of error that are generally of interest ($P_e < 1/4$), the probability of error can be closely approximated by $\tilde{R}^{-1}$, where the S/N of the hard-limiter input

$$\tilde{R} = \frac{\mathcal{E}[\mathrm{tr}^2\ \{K(\xi)Q\}]}{\mathcal{E}[|K(\xi)|]}\ . \tag{79}$$

The mathematical justification of this approximation for any system of this type is essentially identical to the preceding justification for the BAPSK system.

† Standard differential phase-shift-keyed, adaptive-differential phase-shift-keyed, and frequency-shift-keyed systems, as well as adaptive phase-shift-keyed systems, are all of this type.

The quantity $\tilde{R}$ is referred to as the hard-limiter-input S/N throughout this section without any justification being given; this nomenclature can be justified, however. Because the hard-limiter input, $\mathbf{Y}^* Q\mathbf{Y}$, is the sum of the transmitted information digit times a random signal voltage and a random noise voltage,

$$\mathbf{Y}^* Q\mathbf{Y} = I_k^n s + n \quad , \tag{80}$$

the average hard-limiter-input signal strength is

$$\begin{aligned} \mathcal{E}[I_k^n \mathbf{Y}^* Q\mathbf{Y}] &= \mathcal{E}[s] + \mathcal{E}[I_k^n n] \\ &= \mathcal{E}[s] \end{aligned} \tag{81}$$

since $\mathcal{E}[I_k^n n]$ is zero. It has already been shown that

$$\mathcal{E}[s] = \mathcal{E}[\mathrm{tr}\ \{I_k^n K(\xi) Q\}] \tag{82}$$

for a BAPSK system; however, Eq. (82) is true for most systems having a hard-limiter input that is a quadratic form in two Gaussian random variables.

In most systems of this type, the noise portion of the hard-limiter input is zero-mean; thus one must have $\mathcal{E}[n^2]$ to measure the noise power in the hard-limiter input. The average signal-plus-noise power in the hard-limiter input is the sum of the average signal power and the average noise power because

$$\begin{aligned} \mathcal{E}[(I_k^n s + n)^2] &= \mathcal{E}[s^2] + \mathcal{E}[n^2] + 2\mathcal{E}[I_k^n sn] \\ &= \mathcal{E}[s^2] + \mathcal{E}[n^2] \quad . \end{aligned} \tag{83}$$

In most systems of this type for such a Gaussian channel as that described in this report, s is a Rayleigh random variable, and thus

$$\mathcal{E}[s^2] = 3\{\mathcal{E}[s]\}^2 \quad . \tag{84}$$

Hence the average noise power in the hard-limiter input,

$$\mathcal{E}[n^2] = \mathcal{E}[(I_k^n s + n)^2] - 3\mathcal{E}^2[s + I_k^n n] = \mathcal{E}[(\mathbf{Y}^* Q \mathbf{Y})^2] - 3\mathcal{E}^2[I_k^n \mathbf{Y}^* Q \mathbf{Y}] \quad ; \qquad (85)$$

it can be readily verified that

$$\mathcal{E}[(\mathbf{Y}^* Q \mathbf{Y})^2] - 3\mathcal{E}^2[I_k^n \mathbf{Y}^* Q \mathbf{Y}] = 4\mathcal{E}[|K(\xi)|] = \mathcal{E}[n^2] \quad . \qquad (86)$$

Thus $\tilde{R}$ is indeed the hard-limiter-input S/N.

Returning to the evaluation of a BAPSK system probability of error, one can easily show that

$$|K(\xi)| = k_{11}(\xi)k_{22}(\xi) - |k_{12}(\xi)|^2 \qquad (87)$$

and

$$\mathrm{tr}^2\,[K(\xi)Q] = 4\,\mathrm{Im}^2\,\{k_{12}(\xi)\} \quad , \qquad (88)$$

where $\mathrm{Im}\,\{k_{12}(\xi)\}$ is the imaginary part of $k_{12}(\xi)$. After defining the random "correlation field"

$$\mathbf{r}^n_{j_1, j_2} = P^n_{-j_1} P^n_{-j_2} \mathcal{E}[\mathbf{y}^n(-j_1)\mathbf{y}^{n*}(-j_2)|\xi] \quad , \qquad (89)$$

one can easily show that (see Appendix A)

$$|K(\xi)| = \sum_{j_1, j_2 = 1}^{\infty} \exp\,(-\alpha T[j_1 + j_2])\ (\mathbf{r}^n_{0,0}\mathbf{r}^n_{j_1, j_2} - \mathbf{r}^n_{j_1, 0}\mathbf{r}^{n*}_{j_2, 0}) \qquad (90)$$

and

$$\mathrm{tr}^2\,[K(\xi)Q] = 4 \sum_{j_1, j_2 = 1}^{\infty} \exp\,(-\alpha T[j_1 + j_2])\ \mathrm{Im}\,\{\mathbf{r}^n_{j_1, 0}\}\ \mathrm{Im}\,\{\mathbf{r}^n_{j_2, 0}\} \quad ; \qquad (91)$$

the correlation field $\mathbf{r}^n_{j_1, j_2}$, a function of the (random) transmitter state ξ, is defined for integer values of n between one and N and for nonnegative integer values of j_1 and j_2. Thus to evaluate the probability-of-error approximation, Eq. (78), it is necessary to compute the second moments of the correlation field.

In Appendix A, it is shown that for the propagation-medium model of Sec. II,

$$\mathbf{r}^n_{j_1,j_2} = N_0 T \delta_{j_1-j_2} + EG^2T \sum_{k=1}^{K} \sum_{\substack{l_1,l_2,\\ m_1,m_2}} \tilde{\sigma}_k^2 \exp\left(i2\pi\tilde{\lambda}_k[j_1 - j_2]\right)$$

$$\cdot P^n_{-j_1} P^n_{-j_2} \exp\left[\left(i\frac{\pi}{4}[\beta^{n-m_1}_{-j_1-l_1} - \beta^{n-m_2}_{-j_2-l_2}] + i[\phi^{n-m_1} - \phi^{n-m_2}]\right)\right]$$

$$\cdot \exp\left(-i2\pi[m_1 - m_2]\tilde{\tau}_k\right)\tilde{\psi}(\tilde{\tau}_k + l_1, \tilde{\lambda}_k + m_1)\tilde{\psi}^*(\tau_k + l_2, \lambda_k + m_2) \quad , \tag{92}$$

where the channel gain,

$$G^2 = \sum_{k=1}^{K} \sigma_k^2 \quad , \tag{93}$$

the normalized strength of the kth path

$$\tilde{\sigma}_k^2 = \frac{\sigma_k^2}{G^2} \tag{94}$$

the normalized time delay of the kth path

$$\tilde{\tau}_k = \frac{\tau_k - t_0}{T} \quad , \tag{95}$$

the normalized frequency shift of the kth path

$$\tilde{\lambda}_k = \frac{\lambda_k}{1/T} \quad , \tag{96}$$

and

$$\tilde{\psi}(\tilde{\tau},\tilde{\lambda}) = \begin{cases} \exp\left(i\pi\tilde{\lambda}\tilde{\tau}\right)(1 - |\tilde{\tau}|)\, \dfrac{\sin\left(\pi\tilde{\lambda}[1 - |\tilde{\tau}|\right)}{\pi\tilde{\lambda}[1 - |\tilde{\tau}|]}, & |\tilde{\tau}| < 1 \\ 0, & |\tilde{\tau}| \geq 1 \end{cases} \quad . \tag{97}$$

In appendix A, it is also shown that (after neglecting terms smaller than the intersymbol and interchannel interference)

$$\mathcal{E}[|K(\xi)|] = \mathcal{E}[k_{22}(\xi)] \frac{T}{\exp(2\alpha T) - 1} \left\{ N_0 + EG^2 \sum_{k=1}^{K} \tilde{\sigma}_k^2 \cdot \sum_{(l,m)\neq(0,0)} |\tilde{\psi}(\tilde{\tau}_k + l, \tilde{\lambda}_k + m)|^2 \right\} \tag{98}$$

and

$$\mathcal{E}[\mathrm{tr}^2\{K(\xi)Q\}] = E^2G^4T^2 \left| \sum_{k=1}^{K} \tilde{\sigma}_k^2 |\tilde{\psi}(\tilde{\tau}_k, \tilde{\lambda}_k)|^2 \cdot \frac{\exp(\alpha T)\cos(2\pi\tilde{\lambda}_k) - 1}{\exp(2\alpha T) - 2\exp(\alpha T)\cos(2\pi\tilde{\lambda}_k) + 1} \right|^2 \tag{99}$$

where

$$\mathcal{E}[k_{22}(\xi)] = EG^2T \sum_{k=1}^{K} \tilde{\sigma}_k^2 |\tilde{\psi}(\tilde{\tau}_k, \tilde{\lambda}_k)|^2 + N_0T + EG^2T \sum_{k=1}^{K} \tilde{\sigma}_k^2 \sum_{(l,m)\neq(0,0)} |\tilde{\psi}(\tilde{\tau}_k, \tilde{\lambda}_k|^2 \quad . \tag{100}$$

Thus the probability-of-error (approximation)

$$\tilde{P}_e = \frac{1}{2}\left[1 - \left\{1 + 4\frac{\mathcal{E}[|K(\xi)|]}{\mathcal{E}[\mathrm{tr}^2\ [K(\xi)Q]]}\right\}^{-1/2}\right] \quad , \tag{101}$$

where $\mathcal{E}|K(\xi)|$ and $\mathcal{E}\,\mathrm{tr}^2\{K(\xi)\}$ are given by Eqs. (98), (99), and (100).

IV THE PROBABILITY-OF-ERROR EXPRESSION FOR MODIFIED BAPSK SYSTEMS

This section of the report develops a probability-of-error expression (actually an approximation to the probability of error) for modified BAPSK systems. These modifications are the modifications discussed in Sec. VI of Ref. 1. As in Ref. 1, two classes of modifications are considered; the first class consists of modifications to a BAPSK system that can also be employed in systems similar to a BAPSK system, the second class consists of modifications to a BAPSK system that can be employed only in a BAPSK system or a system of comparable sophistication.

A very simple modification, belonging to the first class of modifications, is the adjustment of the subsystem signaling rate. Because the subsystem signaling rate is not a fixed parameter in the error-rate expression, Eq. (101), this BAPSK system modification is already included in the error-rate expression.

Two other simple modifications, which are included in most systems, are time synchronization and frequency synchronization. The synchronization time shift, t_0, of a BAPSK system is very slowly varying, and thus it is essentially constant. Time synchronization is already included in the BAPSK system error-rate expression; as can be readily seen from this expression, the synchronization time shift, t_0, is merely added to the time delays of the individual paths. Frequency synchronization or automatic frequency control (AFC) can be readily included in the BAPSK system error-rate expression. The synchronization frequency shift is so slowly varying that it is essentially constant. Because the synchronization frequency shift is essentially constant, it can be included in the scattering function of the channel by merely adding the synchronization frequency shift to the frequency shifts of the individual paths. (If the noise is not white, the spectrum of the noise must be shifted by the synchronization frequency shift also.) If the time and frequency synchronization of the system are operating perfectly, the center time delay and frequency shift of the propagation medium are zero:

$$\sum_{k=1}^{K} \sigma_k^2 \lambda_k = 0 \qquad (102)$$

$$\sum_{k=1}^{K} \sigma_k^2 \tau_k = 0 \quad . \tag{103}$$

Because the time delays and frequency shifts of the individual paths of the propagation medium are not fixed in the BAPSK system error-rate expression, time and frequency synchronization are already included in the error-rate expression.

For alleviating dispersive self-interference effects caused by time delays, time guard band is one of the most beneficial modifications that can be incorporated into a BAPSK system or similar systems. For a system transmitting signaling elements of length $T + \Delta$ with a time guard band equal to Δ, it can be readily verified that one merely uses in Eq. (101) the values of $\mathcal{E}[|K(\xi)|]$ and $\mathcal{E}[\mathrm{tr}^2[K(\xi)Q]]$ given by Eqs. (B.5), (B.6), and (B.7) of Appendix B. From these expressions it is readily apparent that for time-delay spreads less than Δ, there are no self-interference effects caused by time delays, if the system is properly synchronized.

The addition of diversity receivers is another frequently employed modification in systems like a BAPSK system. The only type of diversity considered in this report is post-detection combining of statistically independent receiver outputs. Only statistically independent receiver outputs are considered because the analysis of statistically dependent diversity receiver outputs is complex and because the probability of error for dependent diversity operation can be bounded by the probability of error for independent diversity operation. The diversity receivers can be displaced in space, frequency, polarization, or time, as long as they are statistically independent.

When the order of diversity is D, it can readily be verified that the conditional probability of error

$$\begin{aligned} P_e(D,\xi) &= \Pr\left\{\sum_{d=1}^{D} I_k^n \mathbf{Y}_d^* \, Q \mathbf{Y}_d < 0\right\} \\ &= \Pr\left\{\frac{\sum_{d=1}^{D} |\mathbf{x}_d|^2}{\sum_{d=1}^{D} |\mathbf{y}_d|^2} < -\frac{\lambda_2(\xi)}{\lambda_1(\xi)}\right\} \quad , \end{aligned} \tag{104}$$

where the subscript d denotes the appropriate diversity receiver, the eigenvalues, λ_1 and λ_2, are given by Eqs. (57) and (58), and the random variables, $\mathbf{x}_k$ and $\mathbf{y}_k$, are statistically independent, complex, Gaussian random variables. However, it is well known that[16]

$$\left(\sum_{d=1}^{D} |\mathbf{x}_d|^2\right) \Big/ \left(\sum_{d=1}^{D} |\mathbf{y}_d|^2\right) = f_{2D}$$

has an F distribution with parameters $m = n = 2D$. Thus the conditional probability of error

$$P_e(D,\xi) = \int_0^{-\lambda_2(\xi)/\lambda_1(\xi)} \frac{\Gamma(2D)}{\Gamma^2(D)} \frac{f^{D-1}}{(1+f)^{2D}} df$$

$$= \frac{\Gamma(2D)}{\Gamma^2(D)} \sum_{j=0}^{D-1} \binom{D-1}{j} (-1)^j \frac{1}{D+j} \left[1 - \left(1 - \frac{\lambda_2(\xi)}{\lambda_1(\xi)}\right)^{-(D+j)}\right], \tag{105}$$

but $P_e(1,\xi) = P_e(\xi) = (1 - \lambda_1(\xi)/\lambda_2(\xi))^{-1}$, and hence [see Appendix B] the conditional probability of error for Dth-order diversity

$$P_e(D,\xi) = \frac{\Gamma(2D)}{\Gamma^2(D)} [P_e(\xi)]^D \left\{1 + \sum_{j=1}^{D-1} \alpha_{D,j} [-P_e(\xi)]^j\right\}, \tag{106}$$

where the constants

$$\alpha_{D,j} = \sum_{l=1}^{D-1} (-1)^{l+D-1} \frac{1}{D+l} \binom{D+l}{l-j} \binom{D-j}{l}. \tag{107}$$

Figure 3 is a plot of $P_e(D,\xi)$ as a function of $P_e(\xi)$.

The unconditional probability of error for a BAPSK system with Dth-order diversity,

$$P_e(D) = \frac{\Gamma(2D)}{\Gamma^2(D)} \left\{\mathcal{E}[(P_e(\xi))^D] + \sum_{j=1}^{D-1} \alpha_{D,j} \mathcal{E}[(-P_e(\xi))^{D+j}]\right\}. \tag{108}$$

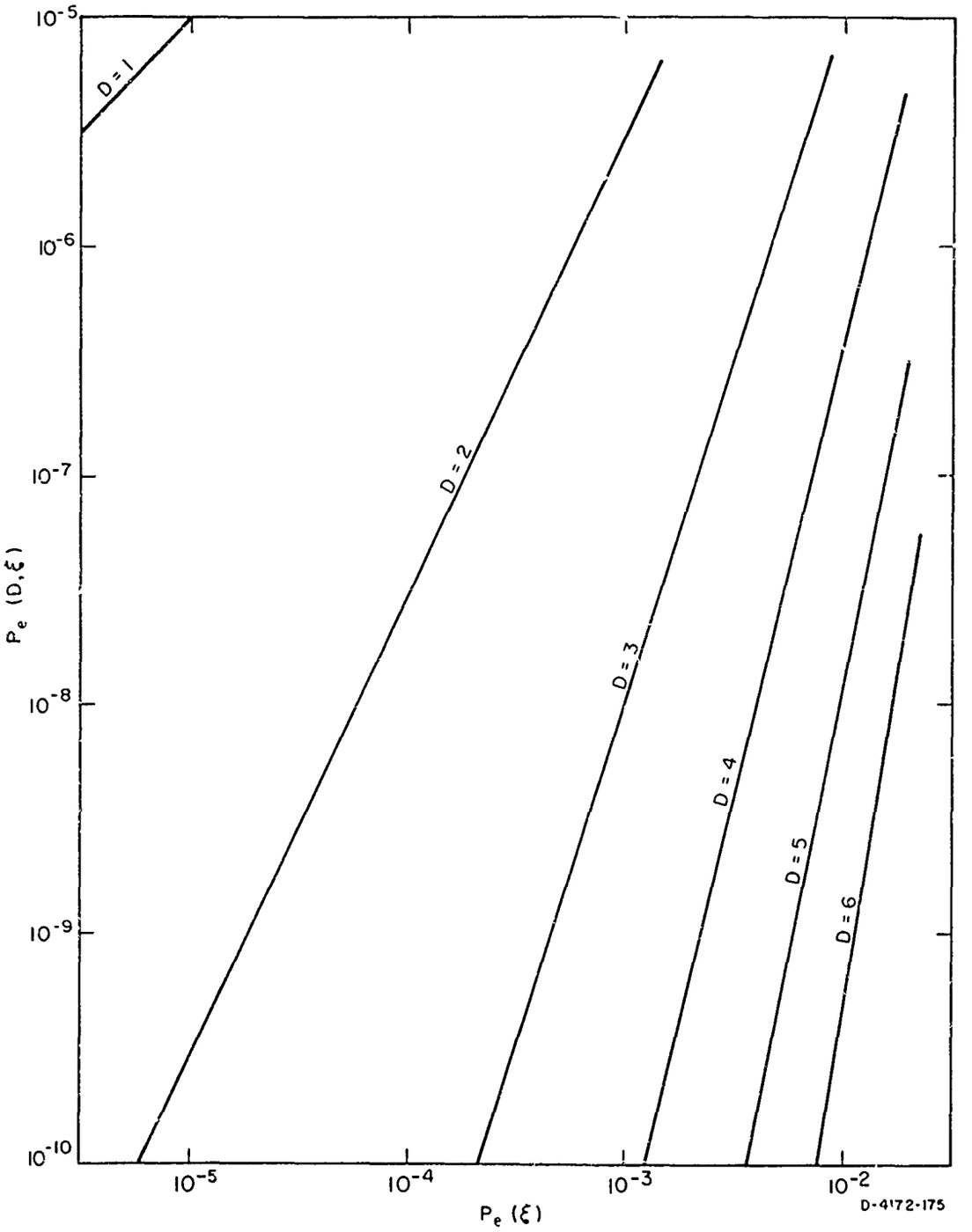

FIG. 3 $P_e(D,\xi)$ AS A FUNCTION OF $P_e(\xi)$

For relatively low orders of diversity and practical values of $P_e(D)$, such that $\alpha_{D,1} P_e \ll 1$

$$P_e(D) \cong \frac{\Gamma(2D)}{\Gamma^2(D)} \mathcal{E}[(P_e(\xi))^D] \quad ; \tag{109}$$

however, by the arguments used in the previous section,

$$P_e(D) \cong \frac{\Gamma(2D)}{\Gamma^2(D)} \frac{\mathcal{E}[|K(\xi)|^D]}{\mathcal{E}^{D/2}\{\mathrm{tr}^2[K(\xi)Q]\}} \quad . \tag{110}$$

By using the Schwartz inequality, it can easily be verified that $\Gamma(2D)/\Gamma^2(D)\ P_e^D D$ is a lower bound on $P_e(D)$. Because $P_e(D,\xi)$ is a deterministic function of $P_e(\xi)$ for any system, this report concentrates primarily on the evaluation of the (unconditional) probability of error for a system without diversity. The benefits accrued by adding diversity are essentially the same for any system.

The transmission of M-ary signals is not included in the error-rate expression. The approach used in this report could be extended to incorporate M-ary signals; this extension would be similar to that used in the analysis of a QDPSK system in Ref. 3.

The second class of modifications are those that can be made only to a BAPSK system. This class of modifications includes alterations to the long-term-average filter characteristic, the division of power between the information-tone and the pilot-tone portions of the transmitted signals, and decision feedback. Other modifications are essentially complete system changes.

The simplest BAPSK system modification (of the second class) is the adjustment of the time constant of the long-term-average filter. This modification is actually only a system adjustment, and since α is not fixed in the probability-of-error expression, it is already included in that expression. Another alteration to the long-term-average filter characteristic is delay compensation (see Sec. VI of Ref. 1). One can include delay compensation in the probability-of-error expression by substituting

$$\mathcal{E}[|K(\xi)|] = \sum_{j_1, j_2=1}^{\infty} \exp\left(-\alpha T[j_1 + j_2]\right) \mathcal{E}\left[\mathbf{r}^n_{jj} \mathbf{r}^n_{j_1, j_2} - \mathbf{r}^n_{j_1, j} \mathbf{r}^{n*}_{j_2, j}\right] \tag{111}$$

and

$$\mathcal{E}[\mathrm{tr}^2[K(\xi)Q]] = 4 \sum_{j_1, j_2=1}^{\infty} \exp\left(-\alpha T[j_1 + j_2]\right) \mathcal{E}[\mathrm{Im}\{r^n_{j_1,j}\}\mathrm{Im}\{r^n_{j_2,j}\}] \qquad (112)$$

in Eq. (101). Delay compensation and a double-pole long-term-average filter can be included by substituting

$$\mathcal{E}[|K(\xi)|] = \sum_{j_1, j_2=1}^{\infty} j_1 j_2 \exp\left(-\alpha T[j_1 + j_2]\right) \mathcal{E}[\mathbf{r}^n_{j,j}\mathbf{r}^n_{j_1,j_2} - \mathbf{r}^n_{j_1,j}\mathbf{r}^{n*}_{j_2,j}] \qquad (113)$$

and

$$\mathcal{E}[\mathrm{tr}^2[K(\xi)Q]] = 4 \sum_{j_1, j_2=1}^{\infty} j_1 j_2 \exp\left(-\alpha T[j_1 + j_2]\right) \mathcal{E}[\mathrm{Im}\{\mathbf{r}^n_{j_1,j}\}\mathrm{Im}\{\mathbf{r}^n_{j_2,j}\}] \qquad (114)$$

in Eq. (101). Similarly, the combination of long-term-average filter outputs of adjacent subsystems and the division of pilot-tone and information-tone power can also be included.

Decision feedback is the only modification that cannot be included easily. The inclusion of decision feedback in the probability-of-error expression would necessitate major theoretical modifications that do not seem justified, because of the unknown value of the modification itself.

V CURVES OF THE PROBABILITY OF BINARY ERROR

The probability of a binary error for basic BAPSK and BDPSK systems (as well as several modified APSK and DPSK systems) is plotted as a function of the S/N in Figs. 4 through 13. In each figure, the curves represent different systems; however, all the curves in each figure are for the same (propagation-medium) scattering function. Different figures display probability-of-error curves for different scattering functions. The expression used in computing the probability of error for various systems is actually the approximation expressed by Eq. (101) of this report.

Time and frequency synchronization, second-order post-detection diversity, and the transmission of quaternary signals by DPSK systems are the only modifications explicitly included in the probability-of-error curves. By proper interpretation of the curves, however one can approximate (or bound) the effects of several other modifications to basic BAPSK and BDPSK systems.

In each figure, the probability-of-error curves labeled K are for a basic BAPSK system, as described in Ref. 1; the curves labeled B are for a basic BDPSK system, as described in Ref. 3. These systems have the same signaling period T, and frequency separation between subsystems $1/T$. The time constant of the BAPSK system long-term-average filter is $\alpha T = 0.1$. This value was chosen, even though it cannot be easily implemented digitally, because it offers a reasonable balance between inherent self-interference and frequency-dispersive effects. A more thorough discussion of the effect of the time constant appears in Sec. VI.

Because the center time shift and frequency shift of each of the scattering functions considered are zero, time and frequency synchronization are essentially included in all systems. The curves labeled $K2$ are for a BAPSK system with second-order, post-detection diversity with statistically independent† diversity inputs. The curves labeled $B2$ are for a BDPSK system with second-order, post-detection diversity with statistically independent diversity inputs. Thus the $K2$ and $B2$ curves are lower bounds on the probability of error of the appropriate system with second-order,

† All diversity inputs are implicitly assumed to be identically distributed in this report.

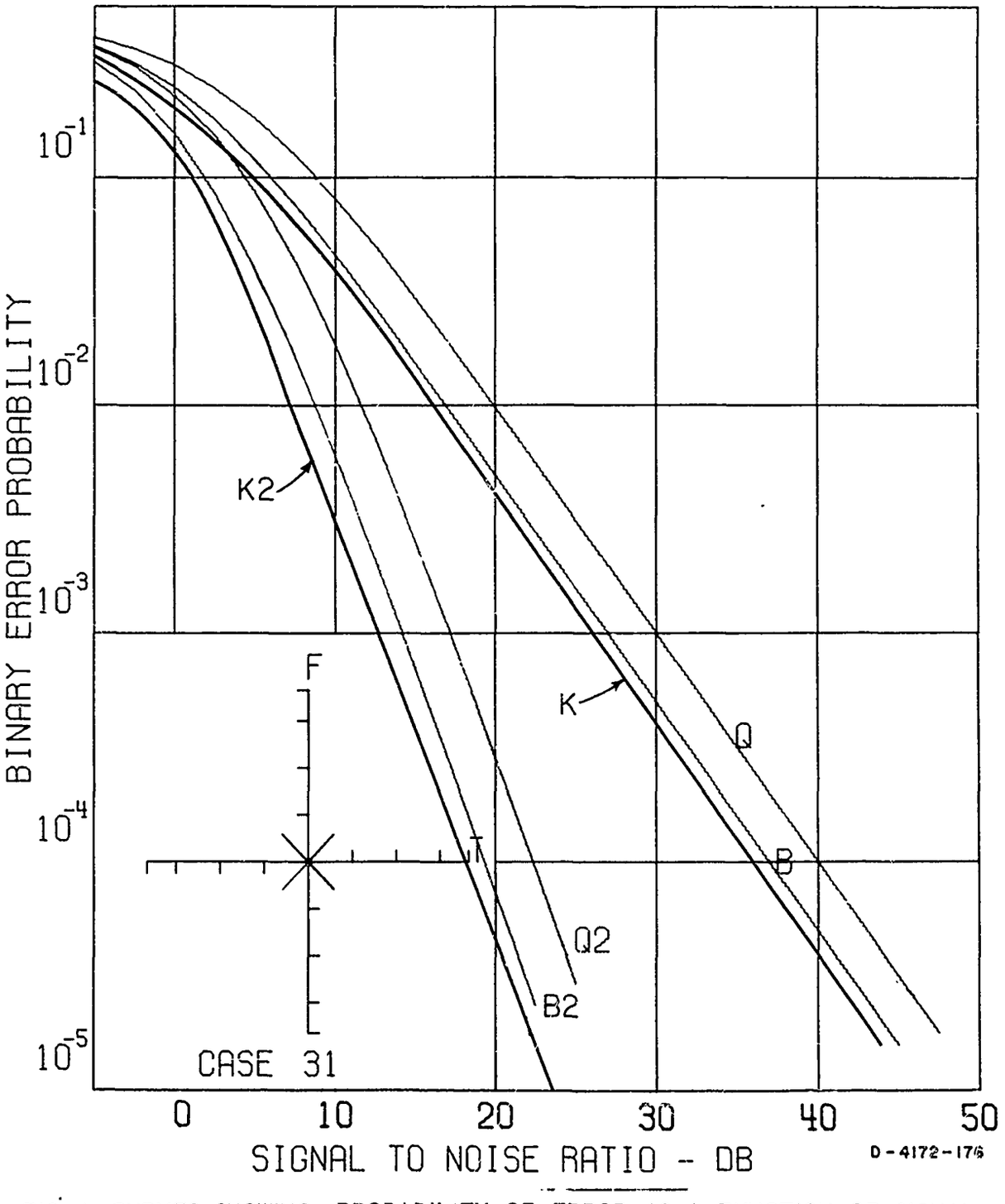

FIG. 4 CURVES SHOWING PROBABILITY OF ERROR AS A FUNCTION OF SIGNAL-TO-NOISE RATIO

Note: All BAPSK system curves are for a fixed time constant (see paragraph 3, p. 35); for a discussion of the effect of changing the time constant, refer to paragraph 2, p. 55.

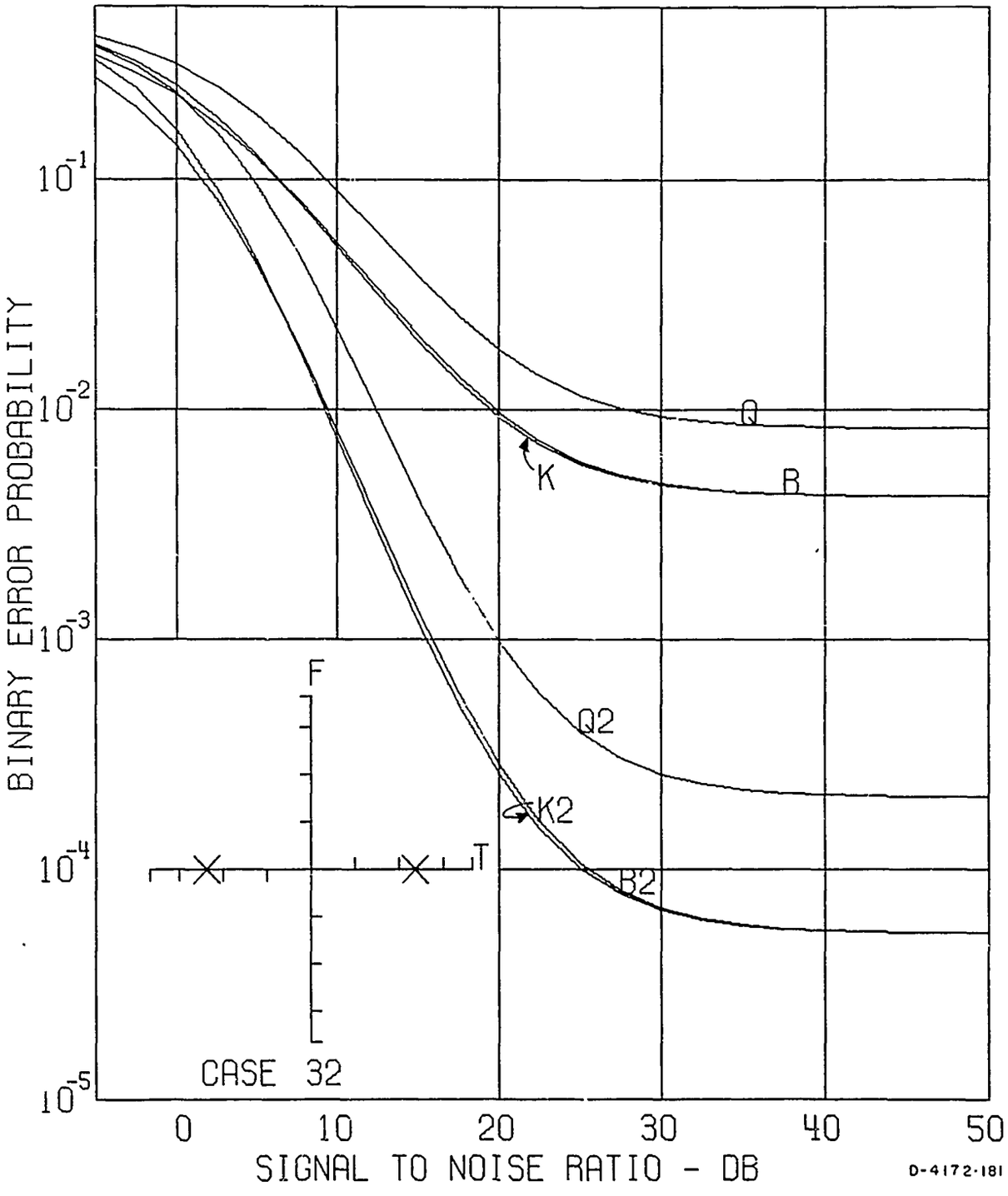

FIG. 5 CURVES SHOWING PROBABILITY OF ERROR AS A FUNCTION OF SIGNAL-TO-NOISE RATIO

Note: All BAPSK system curves are for a fixed time constant (see paragraph 3, p. 35); for a discussion of the effect of changing the time constant, refer to paragraph 2, p. 55.

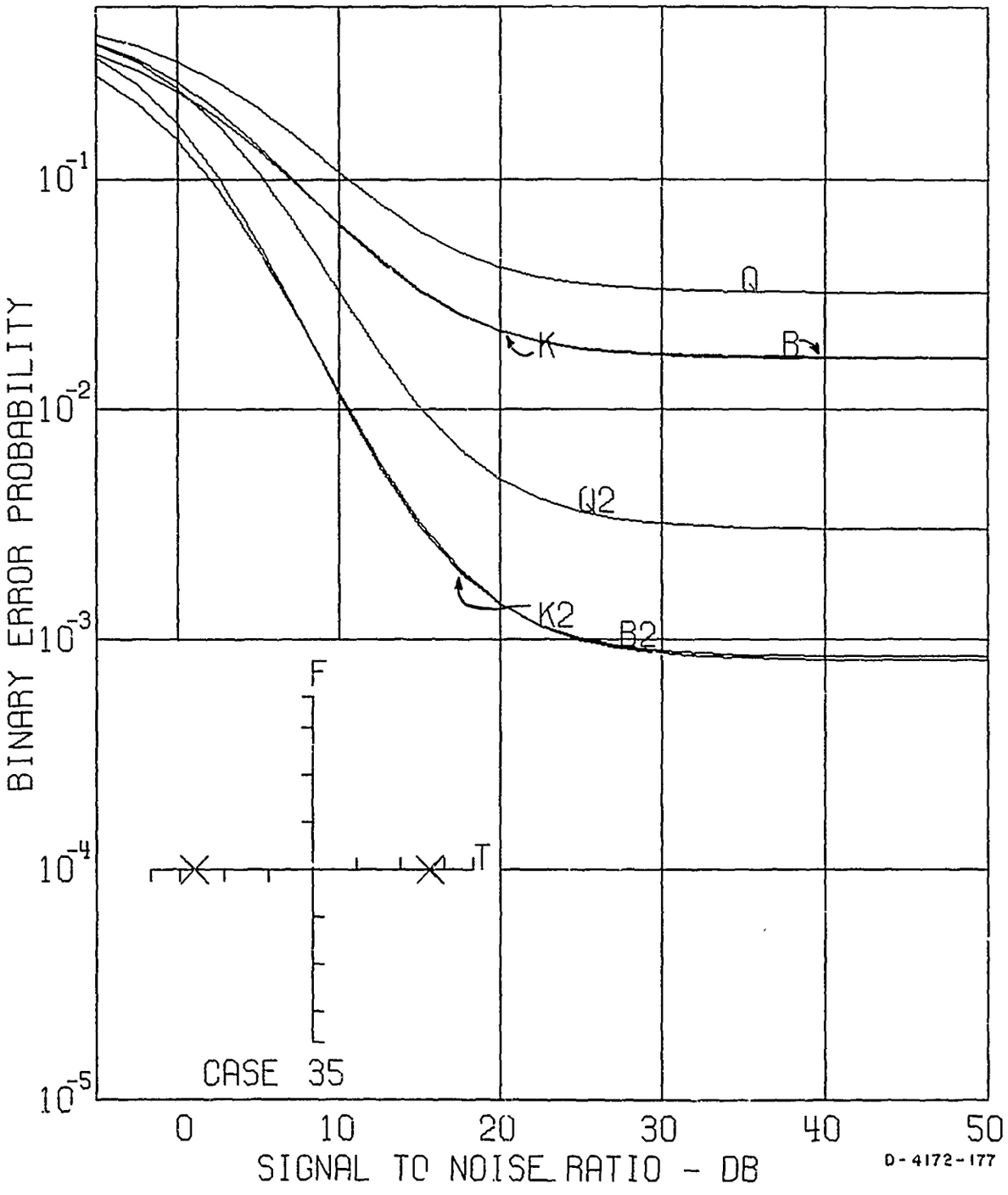

FIG. 6 CURVES SHOWING PROBABILITY OF ERROR AS A FUNCTION OF SIGNAL-TO-NOISE RATIO

Note: All BAPSK system curves are for a fixed time constant (see paragraph 3, p. 35), for a discussion of the effect of changing the time constant, refer to paragraph 2, p. 55.

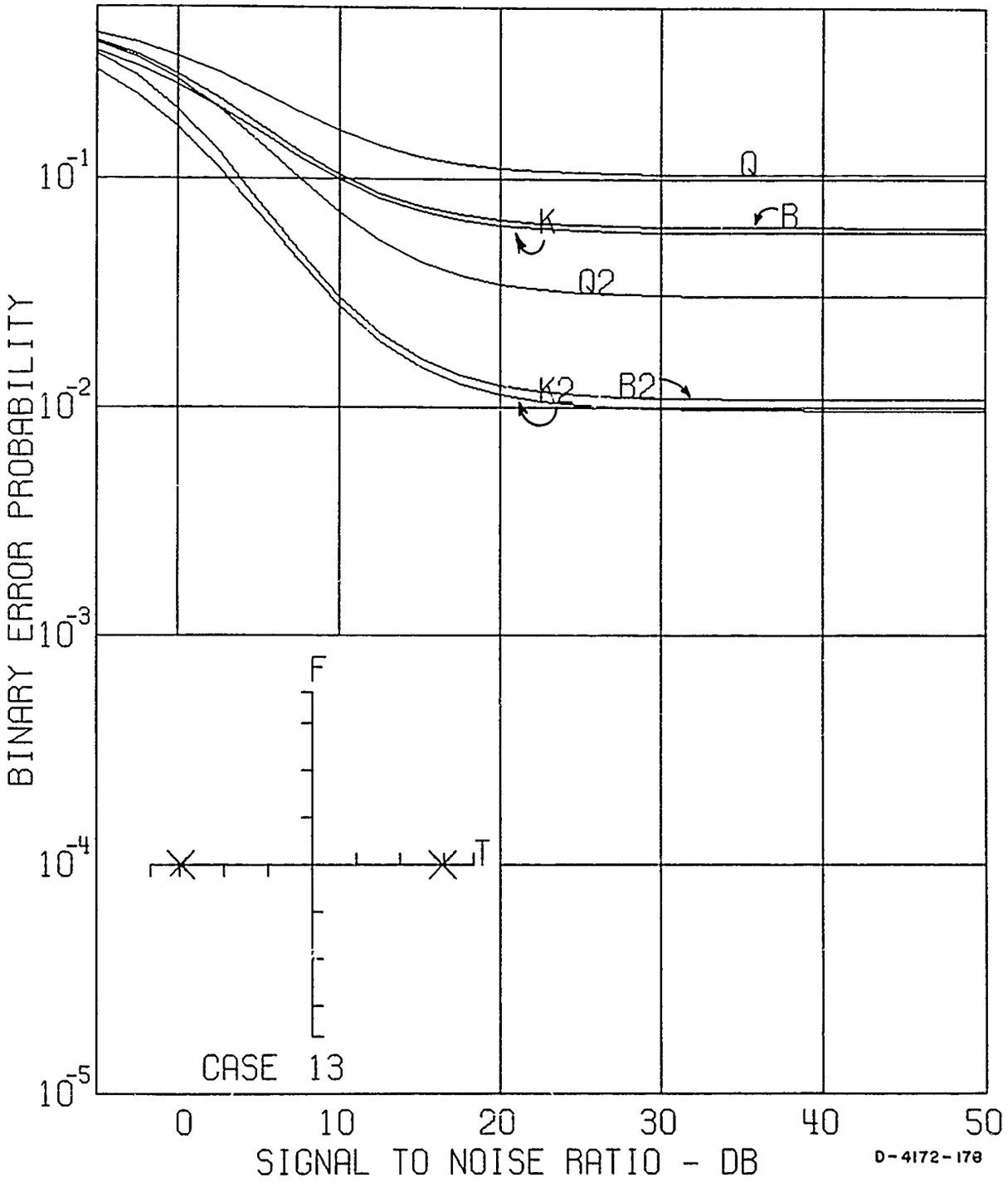

FIG. 7 CURVES SHOWING PROBABILITY OF ERROR AS A FUNCTION OF SIGNAL-TO-NOISE RATIO

Note: All BAPSK system curves are for a fixed time constant (see paragraph 3, p. 35); for a discussion of the effect of changing the time constant, refer to paragraph 2, p. 55.

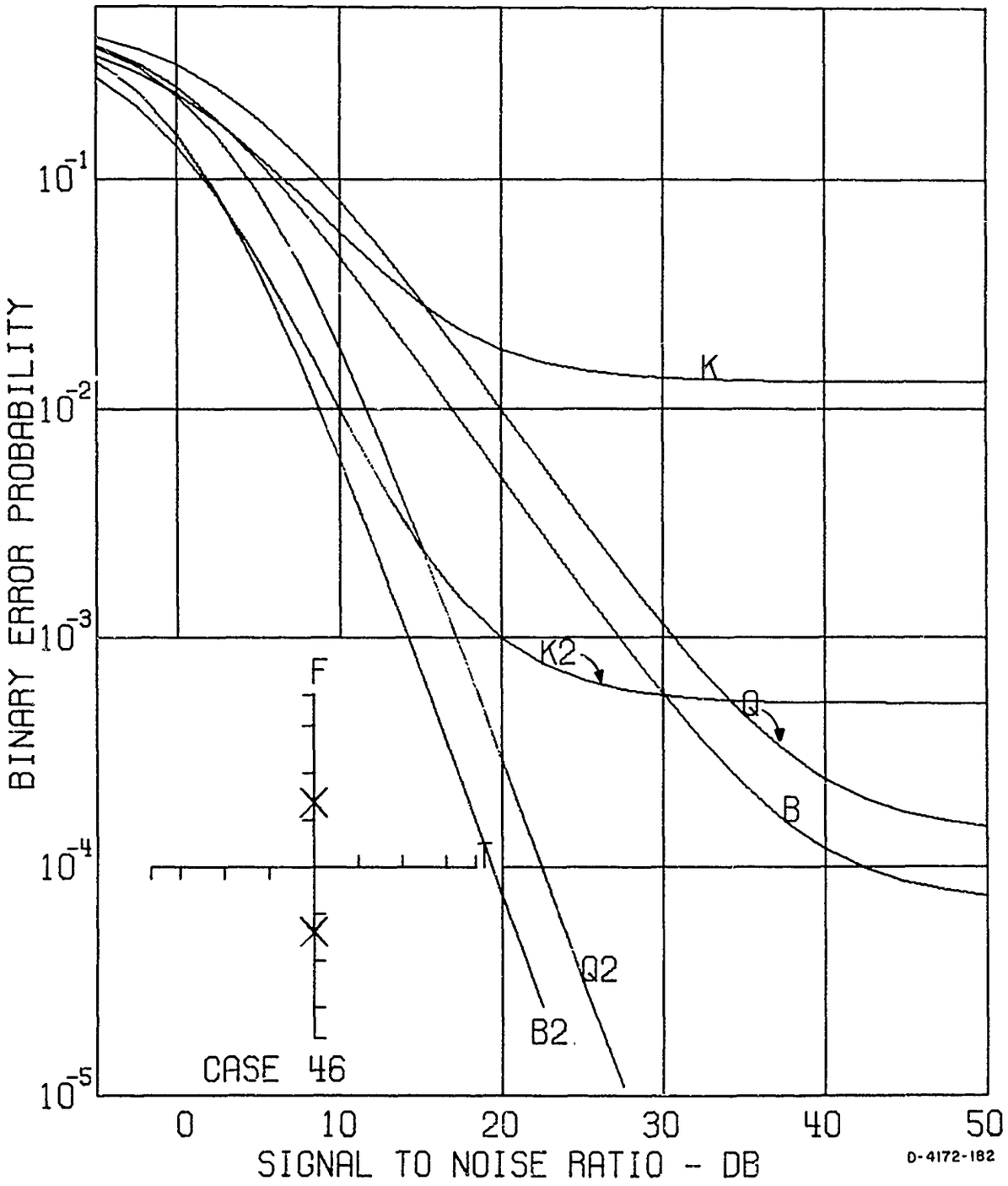

FIG. 8 CURVES SHOWING PROBABILITY OF ERROR AS A FUNCTION OF SIGNAL-TO-NOISE RATIO

Note: All BAPSK system curves are for a fixed time constant (see paragraph 3, p. 35); for a discussion of the effect of changing the time constant, refer to paragraph 2, p. 55.

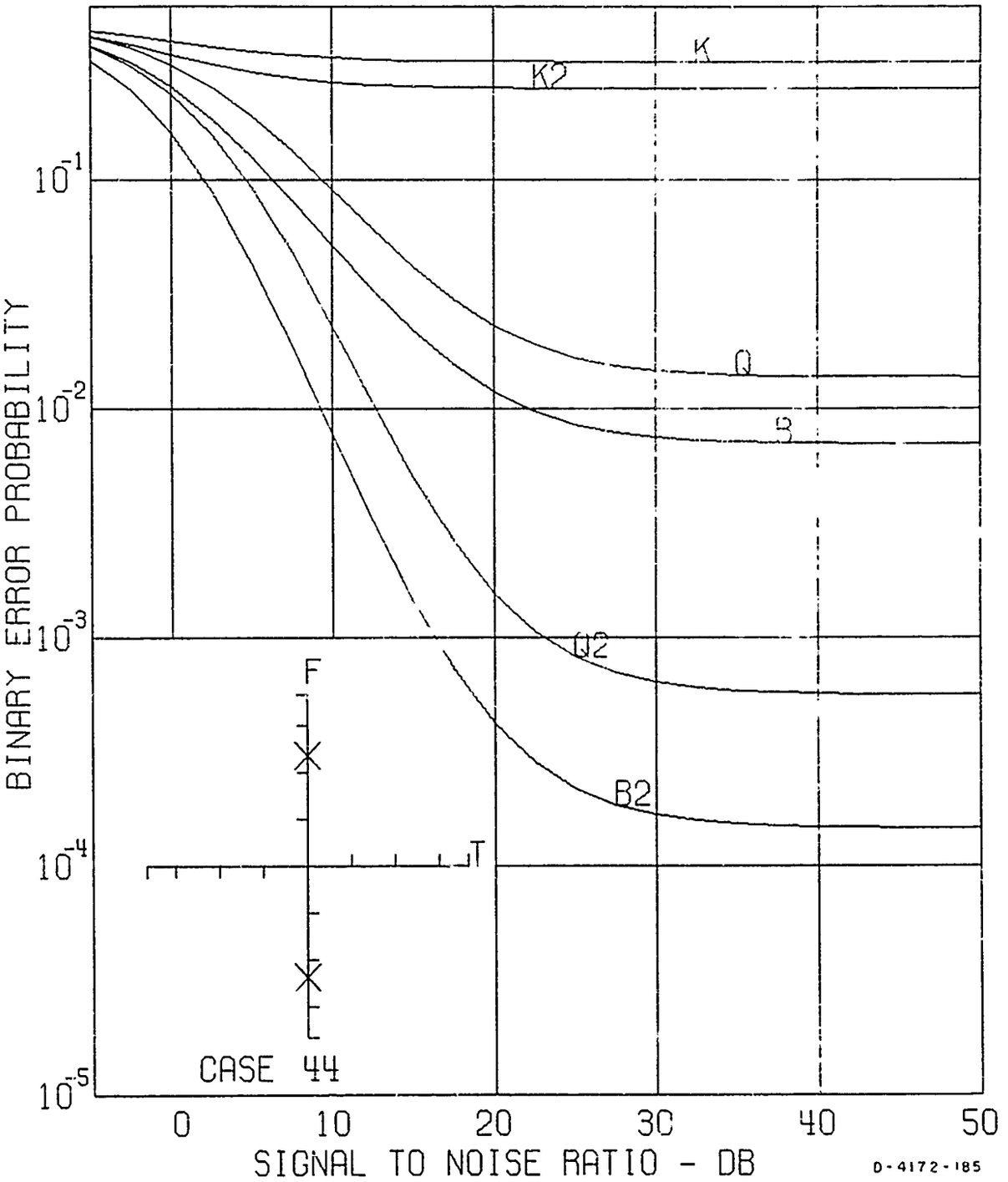

FIG. 9 CURVES SHOWING PROBABILITY OF ERROR AS A FUNCTION OF SIGNAL-TO-NOISE RATIO

Note: All BAPSK system curves are for a fixed time constant (see paragraph 3, p. 35), for a discussion of the effect of changing the time constant, refer to paragraph 2, p. 55.

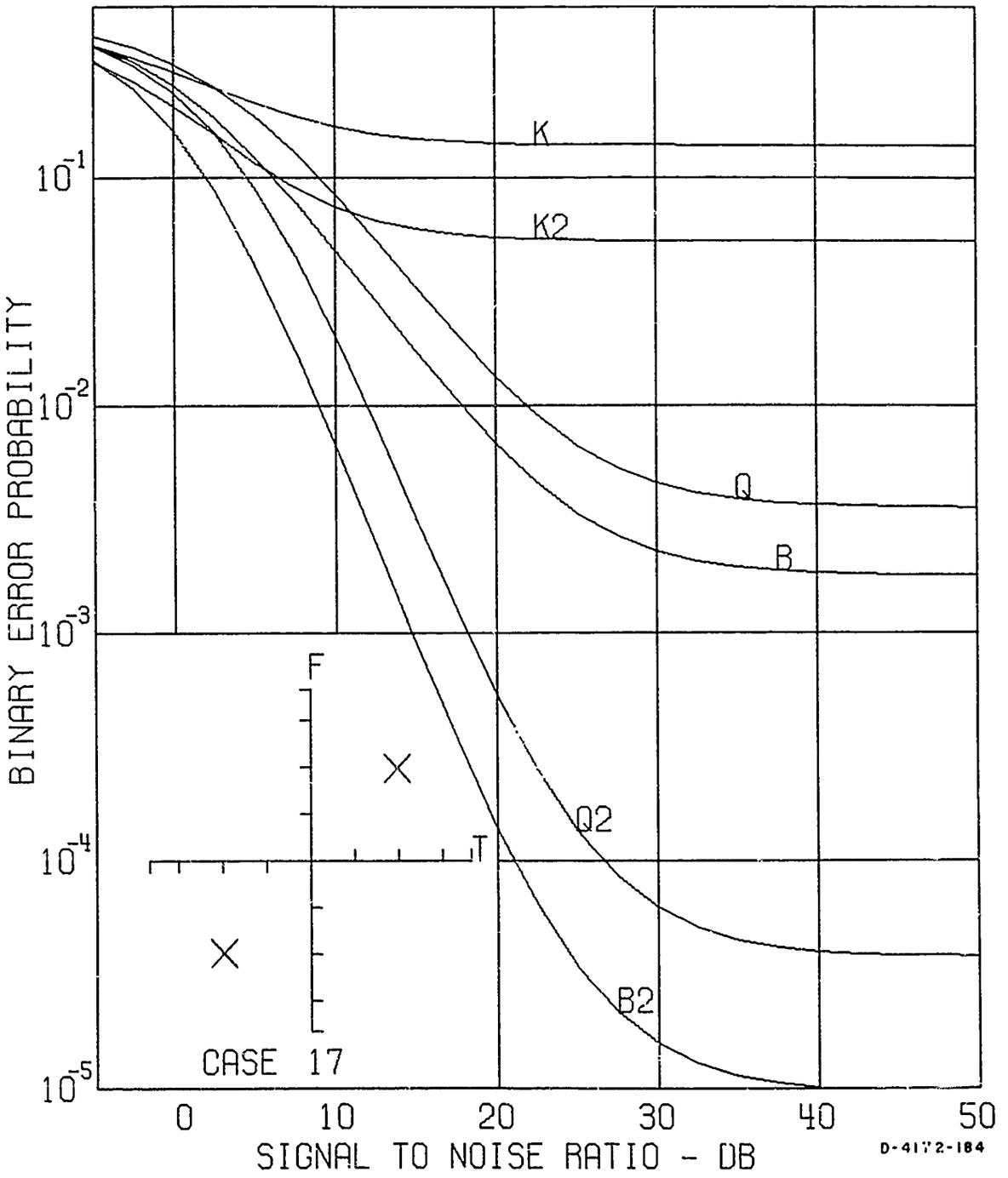

FIG. 10 CURVES SHOWING PROBABILITY OF ERROR AS A FUNCTION OF SIGNAL-TO-NOISE RATIO

Note: All BAPSK system curves are for a fixed time constant (see paragraph 3, p. 35); for a discussion of the effect of changing the time constant, refer to paragraph 2, p. 55.

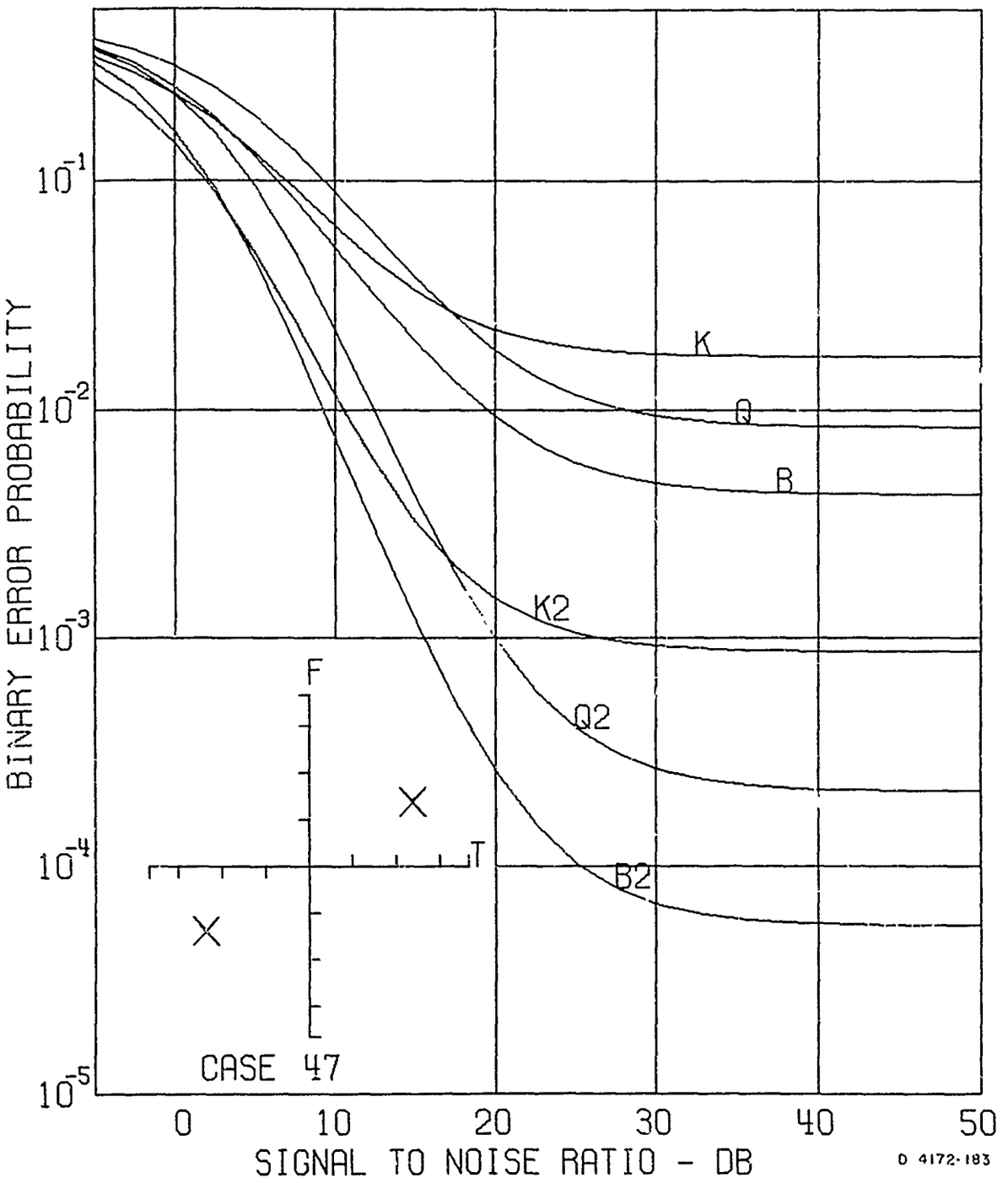

FIG. 11 CURVES SHOWING PROBABILITY OF ERROR AS A FUNCTION OF SIGNAL-TO-NOISE RATIO

Note: All BAPSK system curves are for a fixed time constant (see paragraph 3, p. 35); for a discussion of the effect of changing the time constant, refer to paragraph 2, p. 55.

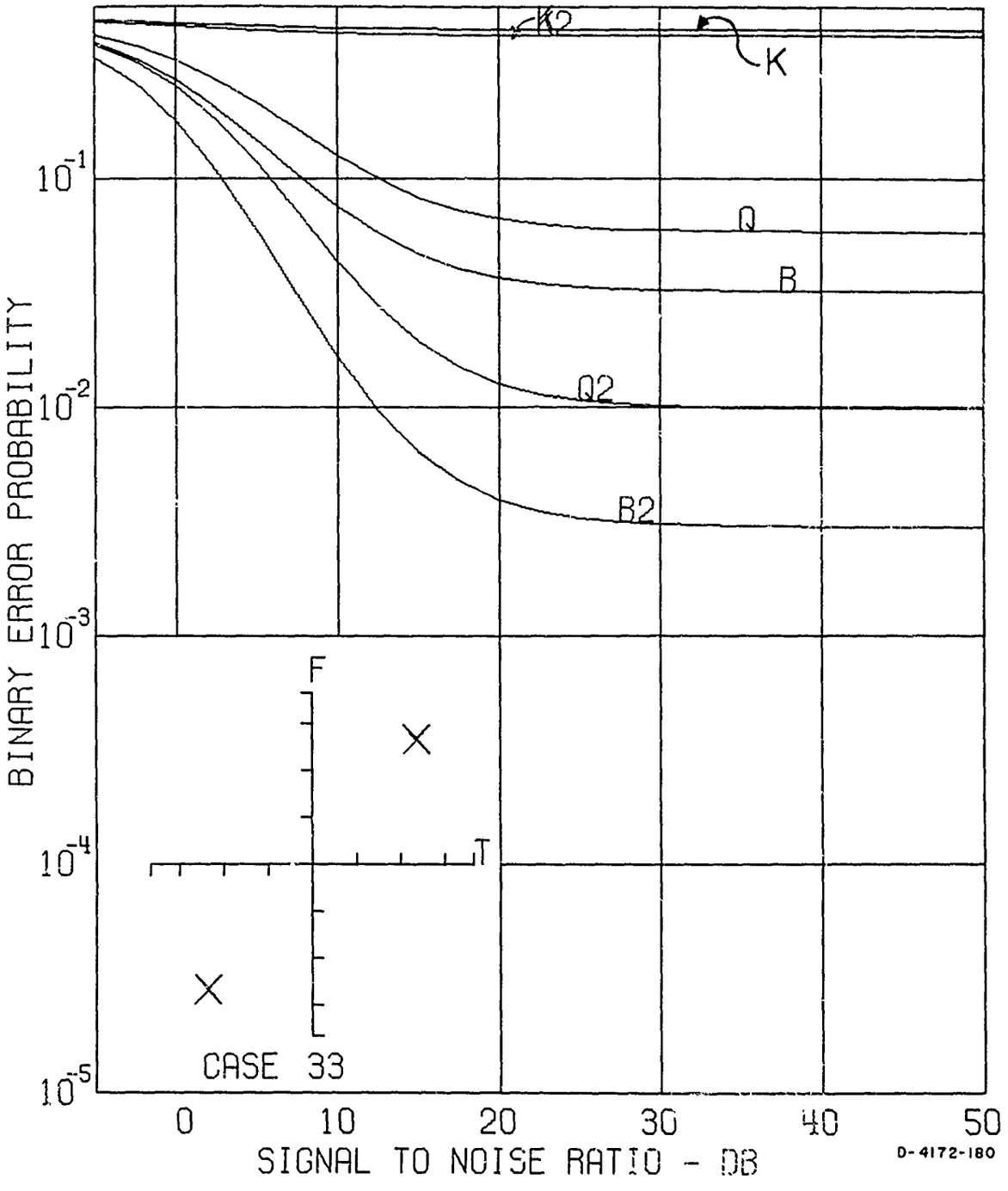

FIG. 12 CURVES SHOWING PROBABILITY OF ERROR AS A FUNCTION OF SIGNAL-TO-NOISE RATIO

Note: All BAPSK system curves are for a fixed time constant (see paragraph 3, p. 35); for a discussion of the effect of changing the time constant, refer to paragraph 2, p. 55.

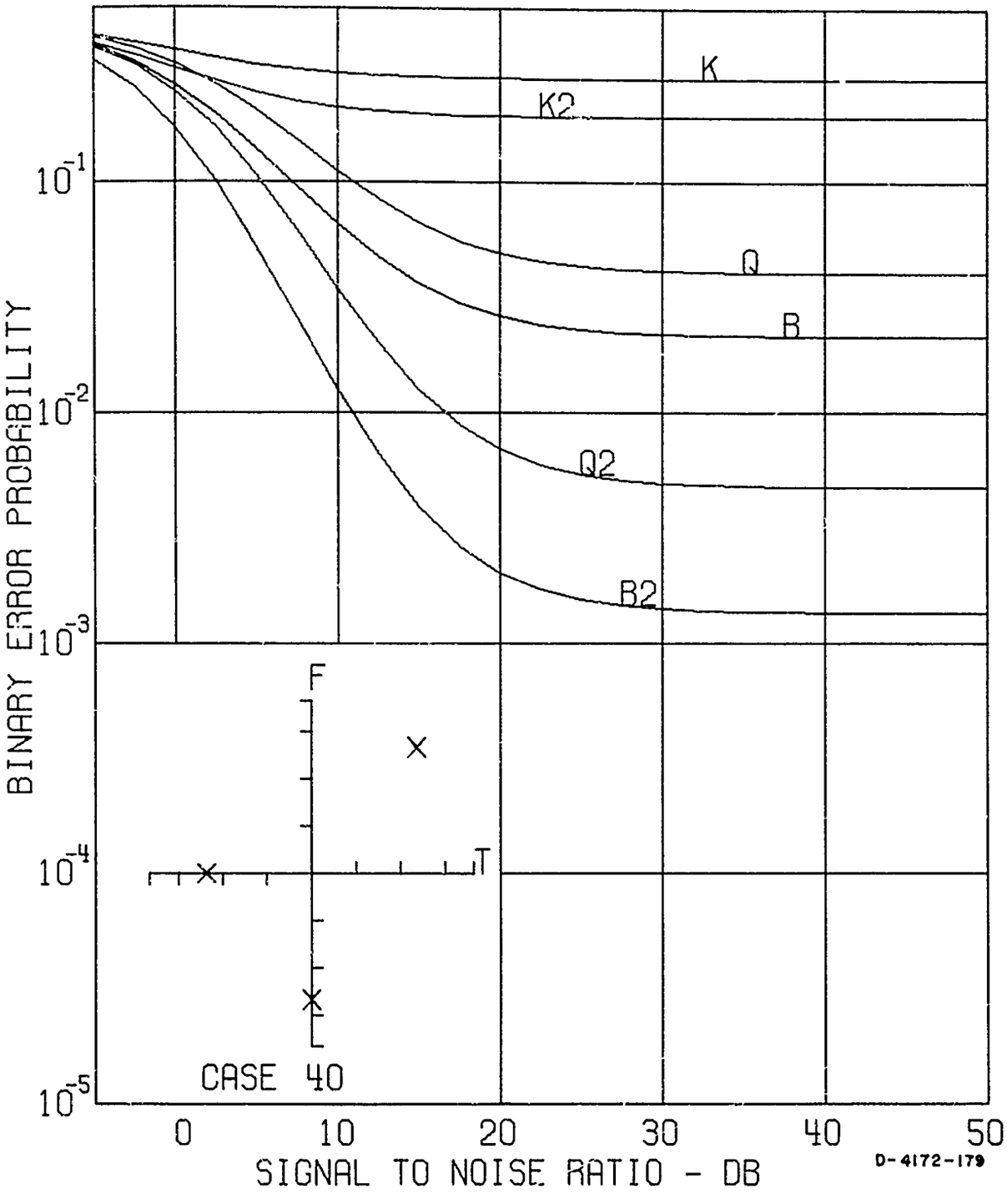

FIG. 13 CURVES SHOWING PROBABILITY OF ERROR AS A FUNCTION OF SIGNAL-TO-NOISE RATIO

Note: All BAPSK system curves are for a fixed time constant (see paragraph 3, p. 35); for a discussion of the effect of changing the time constant, refer to paragraph 2, p. 55.

post-detection diversity; the curves labeled *K* and *B* are upper bounds on the probability of error of the appropriate system with second-order, post-detection diversity.

The curves labeled *Q* are for a DPSK system that transmits two binary digits per signaling element (*i.e.*, a QDPSK system†); the curves labeled *Q2* are for a QDPSK system with second-order, post-detection diversity and statistically independent diversity inputs. The curves labeled *Q* and *Q2* can be interpreted as bounds on the probability of error of a QDPSK system with second-order, post-detection diversity.

Comparison of the *B* and *K* curves seems to be the best method of contrasting APSK and DPSK systems, even though commercially produced systems operate at various signaling rates and incorporate various modifications. If a comparison of the *B* and *K* curves is to be a valid comparison of the basic concepts of the two systems, the systems must have the identical bandwidth, signaling rate, number of subsystems, transmitted signal power, and modifications. For the curves of Figs. 4 through 13 these properties are identical. Neither system employs such modifications as time guard band or *M*-ary signals; modifications of this type should not enhance the performance of one type of system any more than the performance of the other type of system. Perhaps the major inequality in the comparison of the two systems is that various modifications to the long-term-average filter of a BAPSK system are not included. In particular, delay compensation should improve the performance of a BAPSK system significantly.

The curves labeled *Q2* are the probability-of-error curves for a DPSK system transmitting quaternary signaling elements and employing (statistically independent) second-order post-detection diversity. When the outputs of different subreceivers (rather than those of space- or polarization-diversity receivers) are diversity combined, the curves labeled *Q2* are for a system that has the same bandwidth, signaling rate, data transmission rate, and transmitted signal power as the basic BAPSK and BDPSK systems, which have probability-of-error curves labeled *K* and *B*. Thus, contrasting the *B*, *K*, and *Q2* curves offers a valid comparison of these basic systems (actually, the curves labeled *Q2* are for a modified DPSK system). The curves labeled *Q* are for a QDPSK system without diversity; thus they are a bound on the performance of a QDPSK system with second-order post-detection diversity when the diversity inputs are not statistically independent.

† The QDPSK system is described in detail in Ref. 3.

The scattering functions used in computing the curves in the various figures have been normalized. The time delays are normalized by the signaling period, T, of the systems; the frequency shifts are normalized by the frequency separation between adjacent subsystems, $1/T$, of the systems; and the path strengths are normalized by the inverse of the channel power gain,

$$G^{-2} = \frac{1}{\sum_{k=1}^{K} \sigma_k^2} \tag{115}$$

(G^2 is the channel power gain). Thus the probability-of-error curves for a given normalized scattering function,

$$\tilde{S}_H(\lambda,\tau) = \sum_{k=1}^{K} \tilde{\sigma}_k^2 \delta(\lambda - \tilde{\lambda}_k)\delta(\tau - \tilde{\tau}_k) \quad ,$$

are applicable for systems using a signaling period T and a channel with power gain G^2 and an (unnormalized) scattering function

$$S_H(\lambda,\tau) = \sum_{k=1}^{K} \tilde{\sigma}_k^2 G^2 \ \delta(\lambda - \tilde{\lambda}_k/T)\delta(\tau - \tilde{\tau}_k T) \quad . \tag{116}$$

For systems with a signaling period T and a channel power gain G^2, the actual strength of the kth path, $\sigma_k^2 = G^2\tilde{\sigma}_k^2$, is G^2 times the *normalized* strength of the kth path, $\tilde{\sigma}_k^2$; the actual frequency shift of the kth path, $\lambda_k = \tilde{\lambda}_k/T$, is $1/T$ times the *normalized* frequency shift of the kth path, $\tilde{\lambda}_k$; and the *actual* time delay of the kth path, $\tau_k = \tilde{\tau}_k T$, is T times the *normalized* time delay of the kth path, $\tilde{\tau}_k$.

The normalized scattering function is depicted by the plot in the lower-left-hand corner of each figure. For each path, an X is plotted on the T-F plane; the size of the X is proportional to the normalized strength of the path, $\tilde{\sigma}_k^2$; and the center of the X is located at the point

$$(T,F) = (\tilde{\tau}_k, \tilde{\lambda}_k) \quad . \tag{117}$$

To accomodate a wide range of $\tilde{\tau}$ and $\tilde{\lambda}$ values, the T and F axes are logarithmic. In addition to the plot of the normalized scattering function, the parameters of the normalized scattering function, $\{\tilde{\sigma}_k^2, \tilde{\tau}_k, \tilde{\lambda}_k$ for $k = 1, \ldots, K\}$ are tabulated in Table I.

Table I

KEY TO FIGS. 4 THROUGH 13

FIGURE NUMBER	SCATTERING FUNCTION PARAMETERS		
	σ_k^2	τ_k/T	$\lambda_k T$
4	1	0	0
5	1/2 1/2	2.5×10^{-2} -2.5×10^{-2}	0 0
6	1/2 1/2	5×10^{-2} -5×10^{-2}	0 0
7	1/2 1/2	10^{-1} -10^{-1}	0 0
8	1/2 1/2	0 0	2.5×10^{-3} -2.5×10^{-3}
9	1/2 1/2	0 0	2.5×10^{-2} -2.5×10^{-2}
10	1/2 1/2	10^{-2} -10^{-2}	10^{-2} -10^{-2}
11	1/2 1/2	2.5×10^{-2} -2.5×10^{-2}	2.5×10^{-3} -2.5×10^{-3}
12	1/2 1/2	2.5×10^{-2} -2.5×10^{-2}	5×10^{-2} -5×10^{-2}
13	1/3 1/3 1/3	2.5×10^{-2} 0 -2.5×10^{-2}	5×10^{-2} -5×10^{-2} 0

The probability of binary error for each system is plotted as a function of the receiver input S/N (in decibels),

$$(S/N)_{db} = 10 \log_{10}\left(\frac{G^2 E}{N_0}\right) , \quad (118)$$

where the power gain of the channel is $G^2 = \sum_{k=1}^{K} \sigma_k^2$, the channel noise power per unit bandwidth is N_0, and the transmitted system energy per signaling element is E.

The most significant feature of the probability-of-error curves is that the probability of error does not approach zero as the S/N increases (unless there is only one path with no time delay or frequency shift, *i.e.*, a time- and frequency-invariant channel). Careful consideration of the probability-of-error expressions shows that this asymptotic value of the probability of error (as the S/N increases) or residual error $P_e(\infty)$, results from the dispersive self-interference (intersymbol and interchannel interference), the changing (with time) phase shift of the propagation medium, and, in a BAPSK system, the inherent self-interference. To study the sensitivity of the various systems to the dispersive effects that cause this nonzero residual error, it is desirable to have a parameter that is indicative of the performance of the systems and essentially independent of the S/N.

Careful inspection of the probability-of-error curves indicates that the curves are essentially determined by the time- and frequency-invariant probability-of-error curve and the residual error $P_e(\infty)$. Figure 14 illustrates the determination of a probability-of-error curve by the residual error and the time- and frequency-invariant curve. At large values of the S/N, the probability of error is essentially constant and equal to the residual error, because the operation of the system is essentially determined by the energy-scattering effects of the propagation medium. For S/N such that the time- and frequency-invariant probability of error is

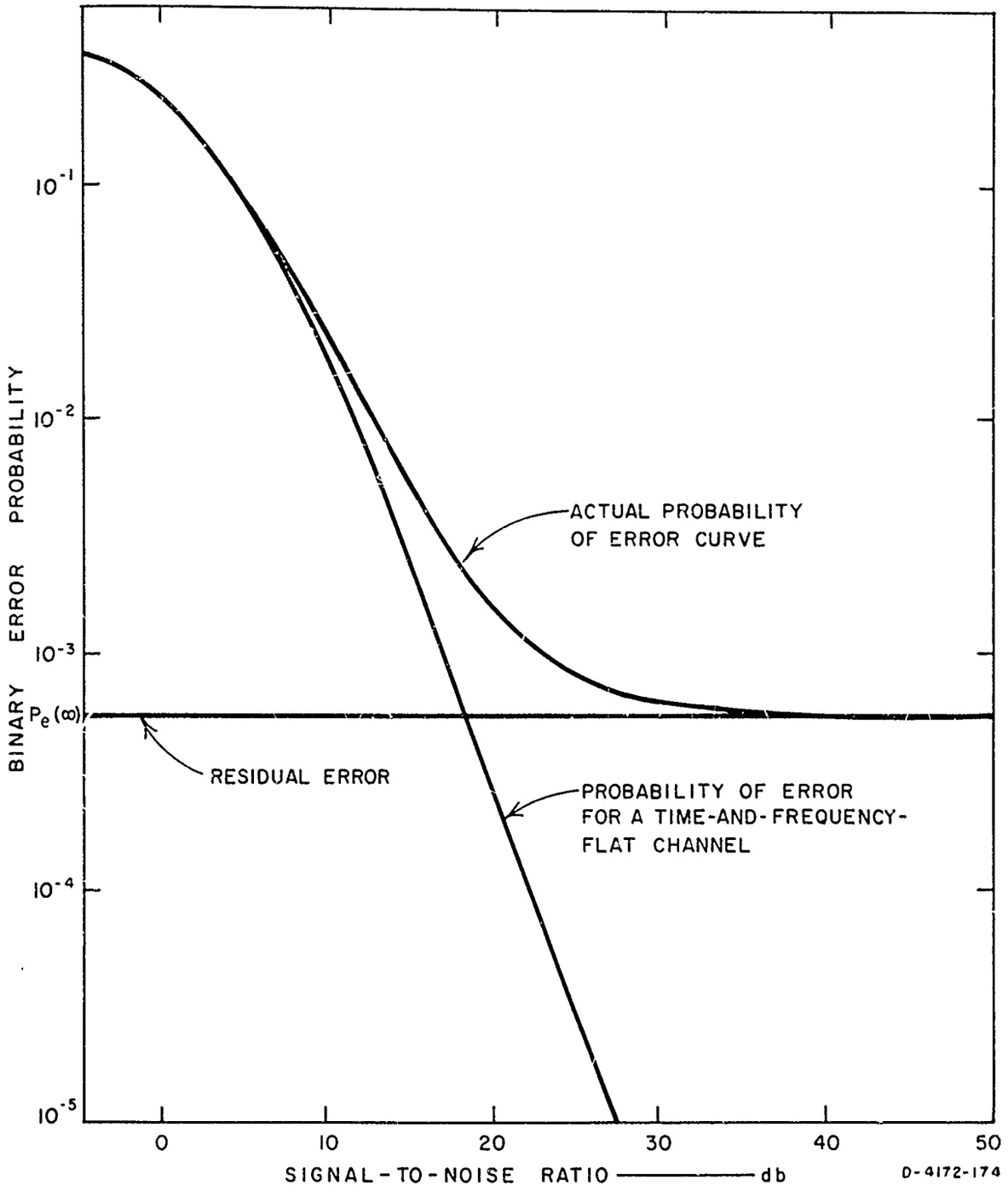

FIG. 14 DETERMINATION OF THE PROBABILITY-OF-ERROR CURVE BY THE RESIDUAL ERROR AND THE FLAT-FLAT PROBABILITY-OF-ERROR CURVE

greater than the residual error, the probability of error is essentially equal to the time- and frequency-invariant probability of error, because the performance of the system is essentially determined by the additive noise (rather than by the dispersive effects). Because the time- and frequency-invariant probability-of-error curve is independent of the residual error, the probability of error for various scattering functions is essentially determined by the residual error. Thus the residual error is a useful parameter for study of the sensitivity of various systems to scattering-function parameters.

Careful analysis of $P_e(\infty)$ for a variety of scattering functions indicates that it is relatively insensitive to the normalized strengths of the paths and the number of paths. The predominant factors determining $P_e(\infty)$ are the maximum differential (normalized) time delay,

$$\Delta\tilde{\tau} = \max_{j,k=1,\ \ldots,\ K} \{|\tilde{\tau}_j - \tilde{\tau}_k|\} \quad , \tag{119}$$

and the maximum differential (normalized) frequency shift,

$$\Delta\tilde{\lambda} = \max_{j,k=1,\ \ldots,\ K} \{|\tilde{\lambda}_j - \tilde{\lambda}_k|\} \quad . \tag{120}$$

When the maximum differential time delay and frequency shift were maintained, $P_e(\infty)$ decreased somewhat as a single path became weaker (*i.e.*, as the normalized path strength decreased) and as the number of paths increased. In addition, for a fixed scattering function with a maximum differential time delay, $\Delta\tilde{\tau}_0$, and maximum differential frequency shift, $\Delta\tilde{\lambda}_0$, $P_e(\infty)$ is essentially equal to the sum of $P_e(\infty)$ for a scattering function with no time delays and maximum differential frequency shift $\Delta\tilde{\lambda}_0$, and $P_e(\infty)$ for a scattering function with no frequency shifts and maximum differential time delay $\Delta\tilde{\tau}_0$. In other words, for the systems considered, the residual error, $P_e(\infty)$, is essentially determined by the maximum differential time delay or the maximum differential frequency shift.

The residual error, $P_e(\infty)$, was calculated for various scattering functions consisting of two equal-strength paths with either zero differential time delay or zero differential frequency shift, so that the sensitivity of the various systems to time delays and frequency shifts could be evaluated. Figure 15 is a plot of $P_e(\infty)$, for scattering functions of this type, as a function of the normalized differential time delay,

$\Delta\tilde{\tau}$, and the normalized differential frequency shift, $\Delta\tilde{\lambda}$. By using the lower horizontal axis, Fig. 15 is a plot of $P_e(\infty)$ as a function of $\Delta\tilde{\lambda}$ for various systems: $K(\lambda)$ denotes a basic BAPSK system: $K2(\lambda)$ denotes a BAPSK system with perfect,† second-order, post-detection diversity. By using the upper horizontal axis, Fig. 15 is a plot of $P_e(\infty)$ as a function of $\Delta\tilde{\tau}$ for various systems: $K(\tau)$ denotes a basic BAPSK system; $K2(\tau)$ denotes a BAPSK system with perfect, second-order, post-detection diversity. The curves for BDPSK and QDPSK systems are the same for both the lower and upper horizontal axes ($\Delta\lambda$ and $\Delta\tau$, respectively). The curve labeled $B[Q]$ is for a $B[Q]$ DPSK system with no diversity; the curve labeled $B2[Q2]$ is for a $B[Q]$ DPSK system with perfect, second-order, post-detection diversity. The curves for BDPSK and QDPSK systems are applicable for use with either horizontal axis; however, the curves for a BAPSK system are applicable for use with only the appropriate horizontal axis. All the BAPSK curves are for a long-term-average filter time constant, $\alpha T = 0.1$.

For a valid comparison of the basic concepts of the systems, the curves labeled $B, K(\lambda)$ or $K(\tau)$, and $Q2$ should be contrasted.

† In this report, perfect diversity implies diversity with statistically independent inputs.

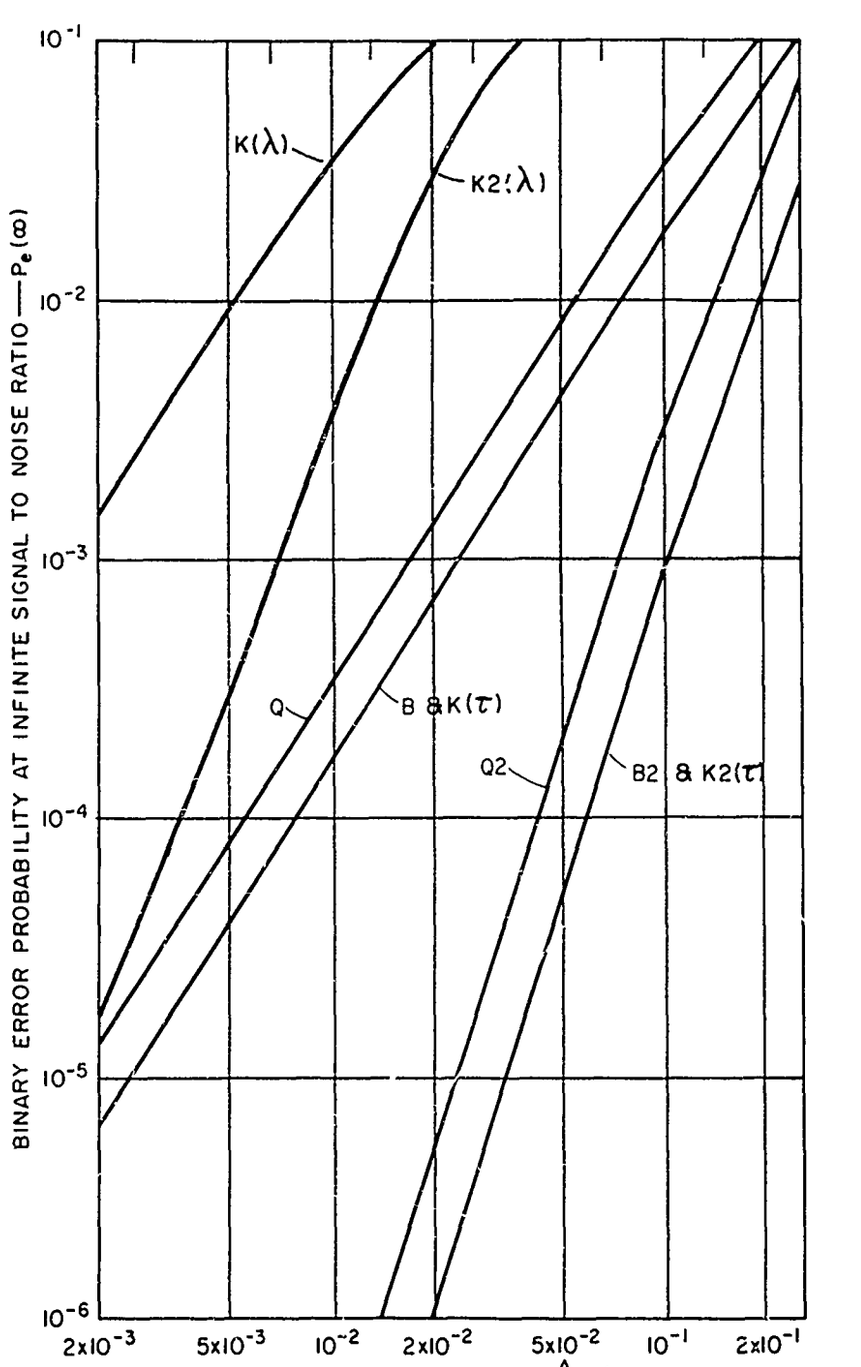

FIG. 15 CURVES SHOWING $P_e(\infty)$ AS A FUNCTION OF DIFFERENTIAL TIME DELAY AND DIFFERENTIAL FREQUENCY SHIFT

Note: All BAPSK system curves are for a fixed time constant (see paragraph 3, p. 35); for a discussion of the effect of changing the time constant, refer to paragraph 2, p. 55.

VI CONCLUSIONS

The relatively simple probability-of-error expression, Eqs. (98) through (101), and the relationship between the probability of error and the S/N at the hard-limiter input, Eqs. (82) and (85), are the most general contributions of this report. Since the probability of error is a monotonic function of the S/N of the hard-limiter input and since it is proportional to the inverse of this S/N for practical values of the probability of error, the relation is intuitively satisfying. Although the probability-of-error expression is developed specifically for a BAPSK system, the techniques employed in developing it are applicable to a large class of digital communications systems. The probability-of-error expression developed in this report is of value, because it is significantly easier to compute than the expressions of other authors. It is interesting to note that the BAPSK system probability-of-error expression is essentially equal to the sum of three other error probabilities (See Fig. 14): the probability of error for a time-and-frequency-invariant propagation medium, the probability of error for a nonadditive (*i.e.*, the additive noise is identically zero) and time-invariant propagation medium, and the probability of error for a nonadditive and frequency-invariant propagation medium.

Another significant, but less general, contribution of this report is the comparison between a basic APSK system and a basic DPSK system presented in the probability-of-error curves of Figs. 4 through 13. As can be readily seen from the curves of Fig. 15, the performance of a basic APSK system (with signaling rate $1/T$) and the performance of a basic DPSK system (with the same signaling rate, $1/T$) are equally sensitive† to time delays; this is not surprising because the time-delay sensitivity results from dispersive intersymbol and interchannel interference primarily, and because both systems are equally prone to dispersive intersymbol and interchannel interference. For a time-and-frequency-invariant propagation medium (or a propagation medium that is dominated by the additive noise) the performance of an APSK system is better than that of a DPSK system. This is to be expected, however, since an APSK system makes its decision (as to whether the transmitted binary information digit was plus or minus

† In this Sec. the performance sensitivity of a system refers to the sensitivity of the probability of binary error for the system. One system is said to be more sensitive than another if the probability of a binary error for the system is larger than the probability of a binary error for the other system.

one) by comparing a noisy matched filter output with a relatively noise-free long-term-average filter output, while a DPSK system makes its decision by comparing two noisy matched-filter outputs. For a time-and-frequency-invariant propagation medium, the performance of an APSK system approaches the performance of a coherent phase-shift-keyed (CPSK) system as the time constant of the long-term-average filter becomes larger; a CPSK system is well known[19] to be the optimum system to combat additive Gaussian noise. Unfortunately, the long-term averaging that makes an APSK system performance approach the performance of a CPSK system for a noise-dominated propagation medium also makes the performance of an APSK system extremely sensitive to variations (with time) of the complex gain of the propagation medium. This performance sensitivity is most readily evidenced by the residual probability of error, Fig. 15, for frequency-invariant propagation mediums. It can readily be seen that the APSK system performance is much more sensitive to frequency shifts than the DPSK system performance. This is reasonable because a DPSK system is prone to complex gain variations during only two signaling intervals, while an APSK is prone to complex gain variations during $1 + \tau_c$ signaling intervals, where τ_c is the time constant (in signaling intervals, T) of the long-term-average filter.

The discussion of the preceding paragraph has been concerned with the comparison of a basic APSK system and a basic DPSK system when both systems have an identical subsystem signaling rate and no modifications (other than time and frequency synchronization), and an APSK system has a long-term-average filter time constant of $\alpha T = 0.1$. Existing APSK and DPSK systems have different subsystem signaling rates and modifications; in addition, the time constant (of the long-term-average filter) of an APSK system is never equal to 0.1. One can glean a great deal of information from the comparison of the preceding paragraph, however.

When an APSK system and a DPSK system have the same signaling rate, the performance of a basic APSK system and the performance of a basic DPSK system are equally sensitive to time-delay effects, while the APSK system performance is *more* sensitive to frequency shifts than that of a DPSK system; thus if one were to pick an optimum subsystem signaling rate for an APSK system, one could always find a DPSK system (*i.e.*, a DPSK system having a subsystem signaling rate equal to that of an APSK system) that would perform at least as well as an APSK system for dispersively dominated propagation mediums.

Hence comparing an APSK system and a DPSK system with the same subsystem signaling rate is not really a constraint. Because most propagation mediums are time-varying, the optimum subsystem signaling rate of the DPSK system would be less than that of the APSK system (it is assumed that the optimum subsystem signaling rate is the rate that makes the system equally sensitive to time-delay and frequency-shift effects). Note that, as shown in Ref. 1, changing the subsystem signaling rate does not change the data transmission rate of the system.

As discussed earlier in this section, the performance of a DPSK system is more sensitive to additive noise than the performance of an APSK system; however, this gain is only for large values of the time constant of the long-term-average filter. Computer calculations of the probability of error for other values of the time constant indicated that, as the time constant becomes small, the noise dominated behavior of an APSK system quickly approaches that of a DPSK system; in addition, increases in $e^{-\alpha T}$ above 10 produce little change in the noise-dominated performance of an APSK system. The same computer calculations also indicated that the time-delay sensitivity of an APSK system is essentially independent of the time constant, and that the frequency-shift sensitivity of an APSK system approaches that of the DPSK system as the time constant is decreased.

The modifications that can be made to both an APSK system and a DPSK system have essentially the same effect. The effect of the addition of perfect dual diversity is indicated by the probability-of-error curves in Figs. 4 through 13. It can readily be seen from these curves that the addition of diversity does not enhance the performance of one system more than the other; however, diversity does enhance the differences in the (nondiversity) performance between the two systems. It can be readily seen from the curves that diversity is a very beneficial system modification.

As noted in Ref. 1, a time guard band is one of the most beneficial system modifications for the purpose of alleviating the effects of dispersive intersymbol and interchannel interference resulting from time delays. In Ref. 3, it is shown for a DPSK system that if the time guard band is Δ, then the effect of all time delays of magnitude less than Δ is essentially negated. From Eqs. (B-5), (B-6), and (B-7) of Appendix B, it is readily apparent that if the time guard band of an APSK system is Δ, then the effect of all time delays of magnitude less than Δ is negated also. This negation of the time-delay effects results in a slight degradation in the S/N and

in the data transmission rate of both a DPSK system and an APSK system. Thus the time guard band modification does not benefit or degrade the performance of the APSK system any more than it does the performance of a DPSK system.

The effect upon the performance of an ADPSK or a DPSK system resulting from the transmission of M-ary signals can be readily inferred by comparing the probability-of-error curves for a QDPSK system and a BDPSK system of Figs. 4 through 13. These curves are for a modified DPSK system; however, the effect of transmitting quaternary information signals in an APSK system should be essentially the same. As indicated by Pierce,[20] diversity combining the independent M-ary subsystems does enhance the system performance, this can be readily seen by comparing the $Q2$ and B probability of error curves in Figs. 4 through 13. A QAPSK system with diversity combining of the outputs of independent subsystems should show the same performance improvement.

Perhaps the major inequality of the system comparison is that several modifications that can be incorporated only into an APSK system are not included. These modifications include alterations to the long-term-average filter [delay compensation, double-pole filter characteristic, and averaging of the outputs of adjacent (in frequency) long-term-average filters], decision feedback, and the division of power between information and pilot tones. Delay compensation is probably the most beneficial of those modifications, and its omission is unfortunate; however, most of these modifications tend only to make the performance of an APSK system approach that of a DPSK system.

APPENDIX A

APPENDIX A

The probability-of-error expression is expressed as a function of $\mathcal{E}[|K(\xi)|]$ and $\mathcal{E}[\mathrm{tr}^2\{K(\xi)Q\}]$ in Eq. (78); thus to evaluate this expression $\mathcal{E}[|K(\xi)|]$ and $\mathcal{E}[\mathrm{tr}^2\{K(\xi)Q\}]$ must be computed. By using the definitions of determinant and trace and the fact that P_0^n is real and $(P_0^n)^2 = 1$, it can readily be verified that

$$\mathcal{E}[|K(\xi)|] = \mathcal{E}[k_{11}(\xi)k_{22}(\xi) - |P_0^n\, k_{12}(\xi)|^2] \tag{A.1}$$

and

$$\mathcal{E}[\mathrm{tr}^2\{K(\xi)Q\}] = 4\mathcal{E}[\mathrm{Im}^2\{P_0^n k_{12}(\xi)\}] \quad , \tag{A.2}$$

where [see Eqs. (28), (40), (41), and (42)]

$$k_{11}(\xi) = \mathcal{E}[|\bar{\mathbf{y}}^n(0)|^2 \,|\xi]$$

$$= \sum_{j_1, j_2=1}^{\infty} \exp\,(-\alpha T[j_1 + j_2])P_{-j_1}^n P_{-j_2}^n \mathcal{E}[\mathbf{y}^n(-j_1)\mathbf{y}^{n*}(-j_2)|\xi] \tag{A.3}$$

$$P_0^n k_{12}(\xi) = P_0^n \mathcal{E}[\bar{\mathbf{y}}^n(0)\mathbf{y}^{n*}(0)|\xi]$$

$$= \sum_{j=1}^{\infty} \exp\,(-\alpha T j)P_{-j}^n P_0^n \mathcal{E}[\mathbf{y}^n(-j)\mathbf{y}^{n*}(0)|\xi] \tag{A.4}$$

and

$$k_{22}(\xi) = P_0^n P_0^n \mathcal{E}[\mathbf{y}^n(0)\mathbf{y}^{n*}(0)|\xi] \quad . \tag{A.5}$$

After introducing the random correlation field

$$\mathbf{r}_{j_1, j_2}^n = P_{-j_1}^n P_{-j_2}^n \mathcal{E}[\mathbf{y}^n(-j_1)\mathbf{y}^{n*}(-j_2)|\xi], \tag{A.6}$$

one finds that

$$\mathcal{E}[|K(\xi)|] = \sum_{j_1, j_2=1}^{\infty} \exp\,(-\alpha T[j_1 + j_2]) \cdot \mathcal{E}[\mathbf{r}_{0,0}^n \mathbf{r}_{j_1, j_2}^n - \mathbf{r}_{0, j_1}^n \mathbf{r}_{0, j_2}^{n*}] \tag{A.7}$$

and

$$\mathcal{E}[\mathrm{tr}^2[K(\xi)Q]] = 4 \sum_{j_1,j_2=1}^{\infty} \exp(-\alpha T[j_1 + j_2]) \cdot \mathcal{E}[\mathrm{Im}\{\mathbf{r}^n_{j_1,0}\}\mathrm{Im}\{\mathbf{r}^n_{j_2,0}\}] \quad . \tag{A.8}$$

Thus to evaluate the probability-of-error expression, one must compute the autocorrelation function of the random correlation field $\mathbf{r}^n_{j_1,j_2}$. Since

$$\mathbf{y}^n(-j) = \int_{-\infty}^{\infty} \mathbf{y}(t) \exp(-i2\pi f_n t)\rho(t + t_0 + jT)dt$$

$$= \int_{-\infty}^{\infty} \mathbf{y}(t)\mathbf{h}^n_j(t)dt \quad , \tag{A.9}$$

where the channel output

$$\mathbf{y}(t) = \int_{-\infty}^{\infty} \mathbf{H}(t,f)\mathbf{X}(f) \exp(i2\pi ft)df + \mathbf{n}(t) \quad , \tag{A.10}$$

the random correlation field

$$\begin{aligned}\mathbf{r}^n_{j_1,j_2} &= P^n_{-j_1} P^n_{-j_2} \Bigg\{ \int\int\int\int_{-\infty}^{\infty} \mathbf{h}^n_{j_1}(t_1)\mathbf{X}(f_1)\mathbf{h}^{n\,*}_{j_2}(t_2)\mathbf{X}^*(f_2) \\ &\quad \cdot R_{\mathbf{H}}(t_2 - t_1, f_2 - f_1) \exp(i2\pi[f_1 t_1 - f_2 t_2])\, dt_1 dt_2 df_1 df_2 \\ &\quad + \int\int_{-\infty}^{\infty} R_n(t_2 - t_1)\mathbf{h}^n_{j_1}(t_1)\mathbf{h}^{n\,*}_{-j_2}(t_2)dt_1 dt_2 \Bigg\} \\ &= P^n_{-j_1} P^n_{-j_2} \Bigg\{ \int\int_{-\infty}^{\infty} S_{\mathbf{H}}(\lambda,\tau)\psi_{\mathbf{h}^n_{j_1}\mathbf{x}^*}(\tau,\lambda) \cdot \psi_{\mathbf{h}^n_{j_2}\mathbf{x}^*}(\tau,\lambda)d\tau d\lambda \\ &\quad + \int_{-\infty}^{\infty} S_{\mathbf{n}}(f)\mathbf{H}^n_{j_1}(f)\mathbf{H}^{n\,*}_{j_2}(f)df \Bigg\} \quad ,\end{aligned} \tag{A.11}$$

where the scattering function of the channel is

$$S_{\mathbf{H}}(\lambda,\tau) = \sum_{k=1}^{K} \sigma_k^2 \delta(\lambda - \lambda_k)\delta(\tau - \tau_k) \tag{A.12}$$

the spectrum of the additive noise is

$$S_{\mathbf{n}}(f) = \begin{cases} N_0, & f \geq 0 \\ 0, & f < 0 \end{cases} \quad , \tag{A.13}$$

the cross-ambiguity function of $\mathbf{x}(t)$ and $\mathbf{y}(t)$

$$\psi_{xy}(\tau,\lambda) = \int_{-\infty}^{\infty} \mathbf{x}\left(t - \frac{\tau}{2}\right) \mathbf{y}^*\left(t + \frac{\tau}{2}\right) \exp(-i2\pi\lambda)\, dt \quad , \tag{A.14}$$

and the Fourier transform of $\mathbf{h}_j^n(t)$ is $\mathbf{H}_j^n(f)$. Because of the special nature of the channel scattering function and the spectrum of the additive noise, the correlation field

$$\mathbf{r}_{j_1,j_2}^n = P_{-j_1}^n P_{-j_2}^n \left\{ N_0 \psi_{\mathbf{h}_{j_1}^n \mathbf{h}_{j_2}^n}(0,0) + \sum_{k=1}^{K} \sigma_k^2 \psi_{\mathbf{h}_{j_1}^n \mathbf{x}^*}(\tau_k,\lambda_k) \psi^*_{\mathbf{h}_{j_2}^n \mathbf{x}^*}(\tau_k,\lambda_k) \right\} \tag{A.15}$$

Because the matched filters of the receiver are orthogonal, *i.e.*,

$$\psi_{\mathbf{h}_{j_1}^n \mathbf{h}_{j_2}^n}(0,0) = \begin{cases} T, & j_1 = j_2 \\ 0, & j_1 \neq j_2 \end{cases} = T\delta_{j_1-j_2} \quad , \tag{A.16}$$

the correlation field

$$\mathbf{r}_{j_1,j_2}^n = N_0 T \delta_{j_1-j_2} + \sum_{k=1}^{K} \sigma_k^2 P_{-j_1}^n P_{-j_2}^n \psi_{\mathbf{h}_{j_1}^n \mathbf{x}^*}(\tau_k,\lambda_k) \cdot \psi^*_{\mathbf{h}_{j_2}^n \mathbf{x}^*}(\tau_k,\lambda_k) \quad . \tag{A.17}$$

The essential problem remaining in the computation of the autocorrelation function of $\mathbf{r}_{j_1,j_2}^n$ is the evaluation of

$$P_{-j}^n \psi_{\mathbf{h}_j^n \mathbf{x}^*}(\tau,\lambda) = \int_{-\infty}^{\infty} \exp\left(-i2\pi\left[f_0 + \frac{n}{T}\right]\left[t - \frac{\tau}{2}\right]\right) \cdot \rho\left(t - \frac{\tau}{2} + t_0 + jT\right) \mathbf{x}\left(t + \frac{\tau}{2}\right) \exp(-i2\pi\lambda t)\, dt \; ; \tag{A.18}$$

however, by using the definition of $\mathbf{x}(t)$ [Eq. (11) of Ref. 1], one finds that

$$P_{-j}^n \psi_{\mathbf{h}_j^n \mathbf{x}^*}(\tau,\lambda) = \sqrt{\frac{E}{T}} \sum_{l_1,m_1} P_{-j}^n \exp\left(i\left[\frac{\pi}{4}\beta_{l_1}^{m_1} + \phi^{m_1}\right]\right) \cdot \exp\left(i2\pi\left[f_0 + \frac{n+m_1}{2T}\right]\tau\right) \int_{-\infty}^{\infty} \rho\left(t_1 - \frac{\tau}{2} + t_0 + jT\right) \rho\left(t_1 + \frac{\tau}{2} - l_1 T\right) \cdot \exp\left(-i2\pi\left[\lambda + \frac{n-m_1}{T}\right]t_1\right) \tag{A.19}$$

and by making the substitutions

$$t_1 = t + \frac{t_0}{2} + \frac{l_1 - j}{2} T, \quad l_1 = -j - l$$

and

$$m_1 = n - m,$$

one finds that

$$P^n_{-j}\psi_{h^n_j x^*}(\tau,\lambda) = \sqrt{\frac{E}{T}} \exp\left(-i\pi\lambda\tau + i2\pi\left[f_0 + \frac{n}{T}\right]\tau + i2\pi\lambda Tj + i2\pi\lambda t_0\right)$$

$$\cdot \sum_{l,m} P^{n-m}_{-j-l} \exp\left(i\frac{\pi}{4}\beta^{n-m}_{-j-l} + i\phi^{n-m}\right)$$

$$\cdot \exp\left(i2\pi\frac{m}{T}[\tau - t_0] + i\pi[\tau - t_0 + lT]\left[\lambda + \frac{m}{T}\right]\right)$$

$$\cdot \int_{-\infty}^{\infty} \rho\left(t - \frac{\tau - t_0 + lT}{2}\right)\rho\left(t + \frac{\tau - t_0 + lT}{2}\right)\exp\left(-i2\pi\left[\lambda + \frac{m}{T}\right]t\right) dt. \tag{A.20}$$

After performing the integration in Eq. (A.20), one finds that

$$P^n_{-j}\psi_{h^n_j x^*}(\tau,\lambda) = \sqrt{ET}\exp\left(i2\pi\left[\left(f_0 + \frac{n}{T}\right)\tau + \lambda(jT + t_0) - \frac{\lambda\tau}{2}\right]\right)$$

$$\cdot \sum_{l,m} P^{n-m}_{-j-l} \exp\left(i\frac{\pi}{4}\beta^{n-m}_{-j-l} + i\phi^{n-m}\right)\exp\left(-i2\pi\frac{m}{T}[\tau - t_0]\right)$$

$$\cdot \psi\left(\tau - t_0 + lT,\ \lambda + \frac{m}{T}\right), \tag{A.21}$$

where

$$\psi(\tau,\lambda) = \begin{cases} \exp(i\pi\lambda\tau)\left[1 - \left|\frac{\tau}{T}\right|\right] \dfrac{\sin\left(\pi\lambda T\left[1 - \left|\frac{\tau}{T}\right|\right]\right)}{\pi\lambda T\left[1 - \left|\frac{\tau}{T}\right|\right]}, & \left|\frac{\tau}{T}\right| < 1 \\ 0, & \left|\frac{\tau}{T}\right| \geq 1 \end{cases}, \tag{A.22}$$

and thus the random correlation field

$$\mathbf{r}^n_{j_1,j_2} = TN_0\delta_{j_1-j_2} + TE\sum_{k=1}^{K}\sigma_k^2 \exp\left(i2\pi\lambda_k T[j_1 - j_2]\right)$$

$$\cdot \sum_{\substack{l_1,m_1,\\ l_2,m_2}} P^{n-m_1}_{-j_1-l_1} P^{n-m_2}_{-j_2-l_2} \exp\left(i\frac{\pi}{4}\left[\beta^{n-m_1}_{-j_1-l_1} - \beta^{n-m_2}_{-j_2-l_2}\right] + i[\phi^{n-m_1} - \phi^{n-m_2}]\right)$$

$$\cdot \exp\left(-i2\pi\frac{m_1 - m_2}{T}[\tau - t_0]\right)\psi\left(\tau_k + l_1T,\ \lambda_k + \frac{m_1}{T}\right)\psi^*\left(\tau_k + l_2T, \lambda_k + \frac{m_2}{T}\right). \tag{A.23}$$

For convenience in interpreting later results, it is instructive to compute the mean of the correlation field

$$\mathcal{E}[\mathbf{r}^n_{j_1,j_2}] = \frac{ET}{2}(1 + \delta_{j_1-j_2})\sum_{k=1}^{K}\sigma_k^2\left|\psi(\tau_k,\lambda_k)\right|^2 \cdot \exp\left(i2\pi[j_1 - j_2]\lambda_k T\right)$$

$$+ \delta_{j_1-j_2}\left\{N_0T + ET\sum_{k=1}^{K}\sigma_k^2\sum_{(l,m)\neq(0,0)}\left|\psi\left(\tau_k + lT,\ \lambda_k + \frac{m}{T}\right)\right|^2\right\}. \tag{A.24}$$

In the above expression, the

$$(1/2)\ ET\ (1 + \delta_{j_1-j_2})\sum_{k=1}^{K}\sigma_k^2 \ldots$$

term results form the signal portion of $\mathbf{r}^n_{j_1,j_2}$; the $N_0T\delta_{j_1-j_2}$ term results form the additive-noise portion of $\mathbf{r}^n_{j_1,j_2}$; and the

$$\delta_{j_1-j_2}\ ET\sum_{k=1}^{K}\sigma_k^2 \ldots$$

term results from the dispersive self-interference portion of $\mathbf{r}^n_{j_1,j_2}$. Using Eq. (A.24), one can also compute

$$\mathcal{E}[k_{11}(\xi)] = \sum_{j_1, j_2=1}^{\infty} \exp(-\alpha T[j_1 + j_2])\mathcal{E}[\mathbf{r}^n_{j_1, j_2}]$$

$$= \frac{T}{\exp(2\alpha T) - 1}\left[\exp(\alpha T) E \sum_{k=1}^{K} \sigma_k^2 |\psi(\tau_k, \lambda_k)|^2 \cdot \frac{\exp(\alpha T) - \cos(2\pi\lambda_k T)}{\exp(2\alpha T) - 2\exp(\alpha T)\cos(2\pi\lambda_k T) + 1}\right.$$

$$\left. + N_0 + E \sum_{k=1}^{K} \sigma_k^2 \sum_{(l,m)\neq(0,0)} \left|\psi\left(\tau_k + lT, \lambda_k + \frac{m}{T}\right)\right|^2\right] \tag{A.25}$$

and

$$\mathcal{E}[k_{22}(\xi)] = \mathcal{E}[\mathbf{r}^n_{0,0}]$$

$$= ET \sum_{k=1}^{K} \sigma_k^2 |\psi(\tau_k, \lambda_k)|^2 + N_0 T$$

$$+ ET \sum_{k=1}^{K} \sigma_k^2 \sum_{(l,m)\neq(0,0)} \left|\psi\left(\tau_k + lT, \lambda_k + \frac{m}{T}\right)\right|^2 . \tag{A.26}$$

It can also be readily verified that

$$\mathcal{E}[I_0^n C_0^n \mathrm{tr}\{K(\xi)Q\}] = ET \sum_{k=1}^{K} \cdot \sigma_k^2 |\psi(\tau_k, \lambda_k)|^2 \frac{\exp(\alpha T)\cos(2\pi\lambda_k T) - 1}{\exp(2\alpha T) - 2\exp(\alpha T)\cos(2\pi\lambda_k T) + 1} . \tag{A.27}$$

By neglecting terms that are smaller than the dispersive self-interference terms (and assuming $e^{\alpha T} \tilde{=} 1$), it can be shown that for j_1 and $j_2 > 0$

$$\mathcal{E}[\mathbf{r}^n_{0,0}\mathbf{r}^n_{j_1,j_2} - \mathbf{r}^n_{j_1,0}\mathbf{r}^n_{j_2,0}] = \mathcal{E}[\mathbf{r}^n_{0,0}]\mathcal{E}[\mathbf{r}^n_{j_1,j_2}] - 2(1 + \delta_{j_1-j_2})\mathcal{E}[\mathbf{r}^n_{j_1,0}]\mathcal{E}[\mathbf{r}^n_{j_2,0}] \tag{A.28}$$

and

$$\mathcal{E}[\mathrm{Im}\{\mathbf{r}^n_{j_1,0}\}\mathrm{Im}\{\mathbf{r}^n_{j_2,0}\}] = (1+\delta_{j_1-j_2})\mathcal{E}[\mathbf{r}^n_{j_1,0}]\mathcal{E}[\mathbf{r}^{n\,*}_{j_2,0}] \quad , \tag{A.29}$$

and thus

$$\mathcal{E}[|K(\xi)|] = \mathcal{E}[k_{22}(\xi)]\left\{\frac{T}{e^{2\alpha T}-1}\right\}\left\{N_0 + E\sum_{k=1}^{K}\sigma_k^2 \sum_{(l,m)\neq(0,0)}\left|\psi\left(\tau_k + lT,\ \lambda_k + \frac{m}{T}\right)\right|^2\right\} \tag{A.30}$$

and

$$\mathcal{E}[\mathrm{tr}^2\{K(\xi)Q\}] = \mathcal{E}^2[I_0^n C_0^n\ \mathrm{tr}\ \{K(\xi)Q\}]$$

$$= E^2T^2\left[\sum_{k=1}^{K}\sigma_k^2|\psi(\tau_k,\ \lambda_k)|^2\ \frac{e^{\alpha T}\cos 2\pi\lambda_k T - 1}{e^{2\alpha T} - 2e^{\alpha T}\cos 2\pi\lambda_k T + 1}\right] . \tag{A.31}$$

APPENDIX B

APPENDIX B

For a BAPSK system with time guard band, the transmitted signal is given by Eq. (94) of Ref. 1. It can be readily verified that Eqs. (A.1) through (A.18) of Appendix A are valid for a BAPSK system with time guard band if one uses

$$\hat{\psi}_{h_j^n x^*}(\tau,\lambda) = \sqrt{\frac{ET}{\gamma}} \exp\left(i2\pi\left\{[f_0 T + n]\frac{\tau}{T} - j\gamma\lambda T - \frac{\lambda\tau}{2}\right\}\right)$$

$$\cdot \sum_{l,m} P_{-j-l}^{n-m}\left(i\frac{\pi}{4}\beta_{-j-l}^{n-m} + i\phi^{n-m}\right) \exp\left(-i2\pi mj\gamma - i2\pi m\frac{\tau}{T}\right)$$

$$\cdot \hat{\psi}(\tau + \gamma lT,\ \lambda + mT) \quad , \tag{B.1}$$

where the constant

$$\gamma = \left(1 + \frac{\Delta}{T}\right) \tag{B.2}$$

and

$$\hat{\psi}(\tau,\lambda) = \begin{cases} \dfrac{\sin(\pi\lambda T)}{\pi\lambda T} & , \quad \left|\dfrac{\tau}{T}\right| - \dfrac{\Delta}{2T} \leq 0 \\ \exp\left(i\pi\lambda T\dfrac{\tau}{|\tau|}\left[\left|\dfrac{\tau}{T}\right| - \dfrac{\Delta}{2T}\right]\right)\left[\gamma - \left|\dfrac{\tau}{T}\right|\right]\dfrac{\sin\pi\lambda T\left[\gamma - \left|\dfrac{\tau}{T}\right|\right]}{\pi\lambda T\left[\gamma - \left|\dfrac{\tau}{T}\right|\right]} & , \quad 0 < \left|\dfrac{\tau}{T}\right| - \dfrac{\Delta}{2T} < 1 \\ 0 & , \quad \left|\dfrac{\tau}{T}\right| - \dfrac{\Delta}{2T} > 1 \quad . \end{cases} \tag{B.3}$$

Thus the random correlation field for a BAPSK system with time guard band is

$$\hat{\mathbf{r}}^{n}_{j_1,j_2} = N_0 T\delta_{j_1-j_2} + \frac{ET}{\gamma}\sum_{k=1}^{K}\sigma_k^2 \exp\left(i2\pi\gamma\lambda_k T[j_1 - j_2]\right)$$

$$\cdot \sum_{\substack{l_1,m_1,\\ l_2,m_2}} P^{n-m_1}_{-j_1-l_1} P^{n-m_2}_{-j_2-l_2} \exp\left(i\frac{\pi}{4}\left[\beta^{n-m_1}_{-j_1-l_1} - \beta^{n-m_2}_{-j_2-l_2}\right]\right.$$

$$\left. + i[\phi^{n-m_1} - \phi^{n-m_2}]\right) \exp\left(-i2\pi\gamma[m_1 j_1 - m_2 j_2] - i2\pi\frac{\tau_k}{T}[m_1 - m_2]\right)$$

$$\cdot \hat{\psi}\left(\tau_k + \gamma l_1 T, \lambda_k + \frac{m_1}{T}\right)\hat{\psi}^*\left(\tau_k + \gamma l_2 T; \lambda_k + \frac{m_2}{T}\right) \quad . \tag{B.4}$$

It can also be readily verified that Eq. (101) is valid with

$$\mathcal{E}[|K(\xi)|] = \mathcal{E}[\hat{k}_{22}(\xi)]\frac{T}{\exp(2\gamma\alpha T) - 1}$$

$$\cdot \left\{N_0 + \frac{E}{\gamma}\sum_{k=1}^{K}\sigma_k^2 \sum_{(l,m)\neq(0,0)}\left|\hat{\psi}\left(\tau_k + \gamma l T, \lambda_k + \frac{m}{T}\right)\right|^2\right\}, \tag{B.5}$$

$$\mathcal{E}[\mathrm{tr}^2[K(\xi)Q]] = \frac{E^2T^2}{\gamma^2}\left[\sum_{k=1}^{K}\sigma_k^2|\psi(\tau_k,\lambda_k)|^2\right.$$

$$\left. \cdot \frac{\exp(\gamma\alpha T)\cos(2\pi\gamma\lambda_k T) - 1}{\exp(2\gamma\alpha T) - 2\exp(\gamma\alpha T)\cos(2\pi\gamma\lambda_k T) + 1}\right]^2, \tag{B.6}$$

and

$$\mathcal{E}[\hat{k}_{22}(\xi)] = \frac{ET}{\gamma}\sum_{k=1}^{K}\sigma_k^2|\hat{\psi}(\tau_k\ \lambda_k)|^2 + N_0 T$$

$$+ \frac{ET}{\gamma}\sum_{k=1}^{K}\sigma_k^2 \sum_{(l,m)\neq(0,0)}\left|\hat{\psi}\left(\tau_k + \gamma l T, \lambda_k + \frac{m}{T}\right)\right|^2 \quad . \tag{B.7}$$

In Sec. (IV) of this report, it is shown that the conditional probability of error for a BAPSK system with perfect Dth -order diversity is

$$P_e(D,\xi) = \frac{\Gamma(2D)}{\Gamma^2(D)} \sum_{j=0}^{D-1} \binom{D-1}{j} (-1)^j \binom{1}{D+j} \left[1 - \left(1 - \frac{\lambda_2(\xi)}{\lambda_1(\xi)} \right)^{-(D+j)} \right] \quad ; \quad (B.8)$$

thus the conditional probability of error for the basic BAPSK system

$$P_e(\xi) = P_e(1,\xi) = 1 - \left(1 - \frac{\lambda_2(\xi)}{\lambda_1(\xi)} \right)^{-1}$$

$$= \left(1 - \frac{\lambda_1(\xi)}{\lambda_2(\xi)} \right)^{-1} \quad . \quad (B.9)$$

Using $(1 - \lambda_2(\xi)/\lambda_1(\xi))^{-1} = 1 - P_e(\xi)$ and the binomial expansion theorem, one can easily show that

$$P_e(D,\xi) = \frac{\Gamma(2D)}{\Gamma^2(D)} \sum_{j=0}^{D-1} \binom{D-1}{j} (-1)^j \left(\frac{1}{D+j} \right) \cdot \left[1 - \sum_{k=0}^{D+j} \binom{D+j}{k} \left[-P_e(\xi) \right]^k \right]$$

$$= \frac{\Gamma(2D)}{\Gamma^2(D)} \sum_{j=0}^{D-1} \sum_{k=0}^{D+j} \binom{D-1}{j} \binom{D+j}{k} \frac{(-1)^{j+k+1}}{D+j} [P_e(\xi)]^k$$

$$+ \frac{\Gamma(2D)}{\Gamma^2(D)} \sum_{j=0}^{D-1} \binom{D-1}{j} (-1)^j \frac{1}{D+j} \left[1 - \sum_{k=0}^{D-1} \binom{D+j}{k} \left[-P_e(\xi) \right]^k \right] ;$$

(B.10)

however, it can readily be verified that the second term is zero, and thus

$$P_e(D,\xi) = \frac{\Gamma(2D)}{\Gamma^2(D)} \sum_{j=0}^{D-1} \sum_{k_1=D}^{D+j} \binom{D-1}{j} \binom{D+j}{k_1} \cdot \frac{(-1)^{j+k_1+1}}{D+j} [P_e(\xi)]^{k_1} \quad .$$

(B.11)

By letting $k_1 = k - D$ and by interchanging the order of summation, one finds that

$$P_e(D,\xi) = \frac{\Gamma(2D)}{\Gamma^2(D)} [P_e(\xi)]^D \sum_{k=0}^{D-1} [-P_e(\xi)]^k$$

$$\cdot \sum_{j=0}^{D-1-k} (-1)^{D-1-j} \frac{1}{D+j+k} \binom{D+j+k}{j} \binom{D-1}{j+k} \quad , \qquad (B.12)$$

and since

$$\sum_{j=0}^{D-1} (-1)^{D-1-j} \left(\frac{1}{D+j}\right) \binom{D+j}{j} \binom{D-1}{j} = 1 \quad ,$$

$$P_e(D,\xi) = \frac{\Gamma(2D)}{\Gamma^2(D)} [P_e(\xi)]^D [1 + \sum_{k=1}^{D-1} [-P_e(\xi)]^k \alpha_{D,k}] \quad , \qquad (B.13)$$

where

$$\alpha_{D,k} = \sum_{j=0}^{D-1-k} \frac{(-1)^{D-1-j}}{D+j+k} \binom{D+j+k}{j} \binom{D-1}{j+k} \quad . \qquad (B.14)$$

As particular examples,

$$P_e(2,\xi) = 3P_e^2(\xi) - 2P_e^3(\xi)$$

$$P_e(3,\xi) = 10P_e^3(\xi) - 15P_e^4(\xi) + 6P_e^5(\xi)$$

$$P_e(4,\xi) = 35P_e^4(\xi) - 84P_e^5(\xi) + 70P_e^6(\xi) - 20P_e^7(\xi)$$

$$P_e(5,\xi) = 126P_e^5(\xi) - 420P_e^6(\xi) + 540P_e^7(\xi) - 315P_e^8(\xi) + 70P_e^9(\xi) \quad ,$$

and

$$P_e(6,\xi) = 462P_e^6(\xi) - 1980P_e^7(\xi) + 3465P_e^8(\xi) - 3080P_e^9(\xi)$$
$$+ 1386P_e^{10}(\xi) - 252P_e^{11}(\xi) \quad . \qquad (B.15)$$

REFERENCES

1. N. T. Gaarder, "A Mathematical Model for the Kathryn System," Technical Report 2, Part I, Contract DA 36-039 SC-90859, SRI Project 4172, Stanford Research Institute, Menlo Park, California (April (1965).

2. R. F. Daly, "On Modeling the Time-Varying Frequency-Selective Radio Channel," Technical Report 2, Part II, Contract DA 36-039 SC-90859, SRI Project 4172, Stanford Research Institute, Menlo Park, California (July 1964).

3. N. T. Gaarder, "An Examination of Selected High-Frequency Phase Modulation Techniques," Technical Report 3, Contract DA 36-039 SC-90859, SRI Project 4172, Stanford Research Institute, Menlo Park, California (August 1964).

4. Seymour Stein, "Statistical Characterization of Fading Multipath Channels," Research Report 321, Applied Research Laboratory, Sylvania Electronics Systems, a Division of Sylvania Electric Products, Inc., Waltham, Massachusetts (2 January 1963).

5. P. A. Bello, "Characterization of Randomly Time-Variant Linear Channels," *IEEE Trans.* PGCS-11, pp. 360-393 (December 1963).

6. W. B. Davenport, Jr., and W. L. Root, *An Introduction to the Theory of Random Signals and Noise* (McGraw-Hill Book Company, Inc., New York, N.Y., 1958).

7. D. L. Nielson and G. H. Hagn, "Frequency Transformation Techniques Applied to Oblique-Incidence Ionograms," Research Memorandum 13, Contract DA 36-039 SC-87197, DASA Subtask 938/04-014, SRI Project 3670, Stanford Research Institute, Menlo Park, California (January 1964).

8. R. A. Shepherd, "HF Communication Effects Simulation: Instrumentation and Operation of the Field Experiment," Interim Report 3, Contract DA-36-039 SC 87197, DASA Subtask 938/04-014, SRI Project 3670, Stanford Research Institute, Menlo Park, California (December 1963).

9. K. D. Felperin, D. L. Nielson, and N. T. Gaarder, "Propagation-Related Outages on DCA Circuits—A Field Experiment," Research Memorandum 2, Contract SD-189, SRI Project 4554, Stanford Research Institute, Menlo Park, California (July 1964).

10. G. L. Turin, "Error Probability for Binary Symmetric Ideal Reception Through Nonselective Slow Fading and Noise," *Proc. IRE*, Vol. 46, pp. 1603-1619 (September 1958).

11. B. Elspas, "The Effect of Jamming on Error Probability and Message Intelligibility in Frequency-Shift-Keyed Teletype Communications," Technical Report 4, Contract DA 36-039 SC-66381, SRI Project 2124, Stanford Research Institute, Menlo Park, California (December 1959). SECRET

12. J. G. Lawton, "Theoretical Error Rates of Differentially Coherent Binary and Kineplex Data Transmission Systems," *Proc. IRE*, Vol. 47, pp. 333-334 (February 1959).

13. V. W. Ames, "The Correlation Between Frequency-Selective Fading and Multipath Propagation over an Ionospheric Path," *J. Geophys. Res.*, Vol. 68, No. 3, p. 759 (February 1963).

14. V. W. Ames, "Spatial Properties of Amplitude Fading of Continuous 17-Mc Radio Waves," Technical Report 87, Contract NOnr-255(64), NR 088 019, ARPA Order 196-64, Radio Science Laboratory, Stanford University, Stanford, California (March 1964).

15. F. R. Gantmacher, *The Theory of Matrices*, p. 274 (Chelsea Publishing Company, New York, N.Y., 1959).

16. E. Parzen, *Modern Probability Theory and Its Application*, p. 326, (John Wiley and Sons, Inc., New York, N.Y., 1960).

17. P. A. Bello and B. D. Nelin, "The Effect of Frequency Selective Fading on the Binary Error Probabilities of Incoherent and Differentially Coherent Matched Filter Receivers," *IEEE Trans. PGCS-11*, pp. 170-186 (June 1963).

18. P. A. Bello, "Evaluation of Special Modulation Techniques for Improved System Design," Vols. I and II, Report ICS-64-TR-530, Contract AF 19(628)-3414, ITT Communication Systems, Inc., Paramus, New Jersey (30 June 1964).

19. D. Middleton, *An Introduction to Statistical Communication Theory*, p. 814 (McGraw-Hill Book Company, Inc., New York, N.Y. 1960).

20. J. N. Pierce, "Approximate Error Probabilities for Optimal Diversity Combining," *IEEE Trans. PGCS*-11, pp. 352-354 (September 1963).

STANFORD RESEARCH INSTITUTE

MENLO PARK
CALIFORNIA

Regional Offices and Laboratories

Southern California Laboratories
820 Mission Street
South Pasadena, California 91031

Washington Office
808–17th Street, N.W.
Washington, D.C. 20006

New York Office
270 Park Avenue, Room 1770
New York, New York 10017

Detroit Office
1025 East Maple Road
Birmingham, Michigan 48011

European Office
Pelikanstrasse 37
Zurich 1, Switzerland

Japan Office
Nomura Security Building, 6th Floor
1–1 Nihonbashidori, Chuo-ku
Tokyo, Japan

Retained Representatives

Toronto, Ontario, Canada
Cyril A. Ing
67 Yonge Street, Room 710
Toronto 1, Ontario, Canada

Milan, Italy
Lorenzo Franceschini
Via Macedonio Melloni, 49
Milan, Italy